Stem Cell Research & Therapy

RESEARCH Open Access

The antifibrotic potential of IMT504: modulation of GLAST+Wnt1+bone marrow stromal progenitors and hepatic microenvironment

Maximiliano Borda[1,2†], Romina Sierra[1,2†], María José Cantero[2,3†], Sofía Gómez Bustillo[4], Esteban Juan Fiore[2,3], Gianlucca Giardelli[1,2], Matías Martino Garcet[1,2], María Luz Rebottaro[1], Juan Miguel Bayo Fina[2,3], Máximo Schiavone[1,2], Julia Rubione[5], Mariana Gabriela García[2,3], Alejandro Montaner[4], Guillermo Daniel Mazzolini[2,3] and Jorge Benjamín Aquino[1,2*]

Abstract

Background The immunomodulatory oligodeoxynucleotide (ODN) IMT504 might harbor antifibrotic properties within the liver.

Methods Fibrosis models were induced in mice through thioacetamide (TAA) administration and bile-duct ligation. Cre-loxP mice were utilized to identify GLAST+Wnt1+bone marrow stromal progenitors (BMSPs) and to examine their contribution with cells in the liver. In vivo and in vitro assays; flow-cytometry, immunohistochemistry, and qPCR were conducted.

Results IMT504 demonstrated significant inhibition of liver fibrogenesis progression and reversal of established fibrosis. Early responses to IMT504 involved the suppression of profibrogenic and proinflammatory markers, coupled with an augmentation of hepatocyte proliferation. Additionally, this ODN stimulated the proliferation and mobilization of GLAST+Wnt1+BMSPs, likely amplifying their contribution with endothelial- and hepatocytes-like cells. Moreover, IMT504 significantly modulated the expression levels of Wnt ligands and signaling pathway/target genes specifically within GLAST+Wnt1+BMSPs, with minimal impact on other BMSPs. Intriguingly, both IMT504 and conditioned media from IMT504-pre-treated GLAST+Wnt1+BMSPs shifted the phenotype of fibrotic macrophages, hepatic stellate cells, and hepatocytes, consistent with the potent antifibrotic effects observed.

Conclusion In summary, our findings identify IMT504 as a promising candidate molecule with potent antifibrotic properties, operating through both direct and indirect mechanisms, including the activation of GLAST+Wnt1+BMSPs.

†Maximiliano Borda, Romina Sierra and María José Cantero contributed equally to this work.

*Correspondence:
Jorge Benjamín Aquino
jaquino@austral.edu.ar

Full list of author information is available at the end of the article

Keywords GLAST, Immunomodulation, Wnt, Bone marrow stromal progenitors, Plasticity, Macrophages, Hepatic stellate cells, Hepatocytes, Liver progenitors

Introduction

The mammalian liver possesses a remarkable capacity for regeneration, orchestrated by hepatocytes re-entering cell cycle and/or liver progenitor cells. Constituting 70% of liver cells, hepatocytes are organized in fascicles near sinusoidal capillaries. Previous research, including our own, has demonstrated the potential of mesenchymal stem cells (MSCs) derived from bone marrow (BM) stromal fraction to ameliorate liver fibrosis [1–3]. The BM harbors diverse and heterogeneous stromal subpopulations [4–8], with many perisinusoidal BM stromal cells (BMSCs) extending long processes making contact with hematopoietic cells. Some of them are progenitors (BMSPs), capable of forming adherent colonies [9]. Notably, certain BMSPs exhibit significant plasticity, including contribution with hepatocyte-like cells (HLCs) [3, 9–13].

Recently, a subset of BMSPs expressing the glutamate transporter GLAST has been identified [4, 9]. Interestingly only about 10% of GLAST$^+$ BM stromal cells were traced in *Wnt1*^{Cre}; *Rosa26*^{Tom} mice, and exhibit fibroblast colony-forming unit (CFU-F) characteristics. During liver fibrogenesis or after partial hepatectomy, perisinusoidal GLAST$^+$ Wnt1$^+$ BMSPs have been observed to mobilize into the bloodstream and to likely contribute to endothelial-like cells (ELCs) and HLCs within the liver [9].

Immunomodulatory ODNs are synthetic molecules that stimulate various immune cell types. These synthetic ODNs fall into two primary categories: CpG ODNs and non-CpG ODNs. CpG ODNs contain at least one unmethylated cytosine-guanine (CpG) dinucleotide in a specific context [14]. A class of non-CpG ODNs, denoted as PyNTTTTGT (Py: pyrimidine; N: any nucleotide; T: thymidine; G: guanine), has been described [15]. Incubating rat BM MSCs with IMT504, a prototype of the PyNTTTTGT family class, led to a significant increase in CFU-Fs numbers [16]. Additionally, this ODN was shown to induce the mobilization of stromal progenitors into the bloodstream [16], suggesting its potential clinical application in enhancing regenerative mechanisms and tissue recovery [17]. Indeed, IMT504 was also previously shown to elicit beneficial effects in the context of experimental models of diabetes, pain and multiple sclerosis [18–21]. Rat and bone marrow stromal cells incubated with Alexa-Fluor 488- or Texas red-conjugated IMT504 were found to internalize this compound [20]. However, the mechanisms elicited by IMT504 in BMSPs remains poorly understood.

In this study, we explore the roles of IMT504 in both liver fibrosis development and regression, and its impact on the physiological properties of GLAST$^+$ Wnt1$^+$ BMSPs and of other BMSPs subpopulations.

Materials and methods

Oligodeoxynucleotide

ODN IMT504 with phosphorotioate backbone was purchased from Biosynthesis (Lewisville, TX), purified by high-performance liquid chromatography and assayed by MALDY. Lyophilized ODN IMT504 was diluted in depyrogenated water, assayed for lipopolysaccharide contamination and kept at -20 °C until used. ODN IMT504 sequence is 5′ TCATCATTTTGTCATTTTGTCATT 3′.

Animal models

Wnt1^{Cre} (Jackson stock N° 022501) were bred with *Rosa26*$^{td-Tomato}$ (*Rosa26*^{Tom}; Jackson stock N° 007909). In addition, *GLAST*^{CreERT2} [22] were bred with *Rosa26*$^{td-Tomato}$ (*Rosa26*^{Tom}; Jackson stock N° 007908): these mice were crossbred with CD1 mice in an outbreeding program for more than 20 generations, so they are currently in that genetic background. *GLAST*^{CreERT2}; *Rosa26*^{Tom} mice were s.c. injected with tamoxifen (Tx; Sigma-aldrich; T-5648; 20 mg/mL in corn oil; 50 µl/animal) at postnatal day 2 (P2) or P60.

In the experiments, males and females were used. No animals were excluded (no signs of pain were found). The work has been reported in line with the ARRIVE guidelines 2.0.

In vivo fibrogenesis models

Two models of liver fibrogenesis were established. In the TAA model, *GLAST*^{CreERT2}; *Rosa26*^{Tom} mice (2 months-old) received intraperitoneal injections of TAA; 0.2 mg/g body weight; three times per week) for 2 weeks or 8 weeks [2] (Fig. 1A). The animals were distributed into different boxes at random, and the animals in each box received the same type of treatment. No animals were excluded from the analyses. For histology studies, some mice were subcutaneously injected with IMT504 (0.4 mg/ml; 6 mg/kg/animal) [16] 4 h after the 6th TAA dose. Other animals received 3 doses of IMT504: 4 h after the 6th, 12th and 18th TAA dose. Control (vehicle) and naïve (plus/minus IMT504) conditions were also included. In the bile duct ligation (BDL) model, CD1 mice of the same age were anesthetized with 5% isoflurane and an oxygen flow of 0.5-1.0 l/min. They underwent two ligatures around the common bile duct using silk 6.0 sutures, with a survival period of 2 weeks [23]. Some mice received subcutaneous IMT504 injections (as above) 5 days after BDL. Other CD1 mice were treated with TAA for 2 or 8 weeks,

followed by IMT504 administration (or vehicle, 4 h after the last TAA dose). They were euthanized under 5% isoflurane the following day for qPCR analyses of relevant markers.

For liver regression experiments, CD1 mice were treated with TAA for 8 weeks and some received 1 dose of IMT504 or vehicle, 4 h after the 18th TAA dose. These animals were not further subjected to TAA for 2 weeks (Fig. 2A).

For qPCR analyses, animals were anesthetized and their livers were perfused using a washing buffer (1:25 PBC and EDTA 0.4 mM in distilled water) along with collagenase (C5138, Sigma-Aldrich, St. Louis, MO, USA). The liver tissue was mechanically disaggregated and then filtered using a 40 µm pore cell strainer. A 200 µL suspension of total liver sample was subsequently resuspended in Trizol Reagent (SigmaAldrich Co). For obtaining *samples enriched in hepatocytes*, the samples were allowed to decant for thirty minutes and then 2 cycles of centrifugation (5 minutes, 1000 rpm) were performed afterwards [9]. After isolation, 2×10^5 cells/well were seeded in P6 multiwell plates containing DMEM/F12 with 10% FBS (Gibco) and cultured for 3 h. *For Kupffer cells isolation*, the total liver sample was centrifuged at low speed and 4 °C. The supernatant was recovered and resuspended in 2 mL of RPMI. The resulting cell suspension was subjected to a density gradient using Histodenz (Sigma-Aldrich), with a 30% concentration in PBS. The isolated pellet was seeded in P12 multiwell plates ($2{,}5\times10^6$ cells/well) and incubated with RPMI supplemented with 10% FBS for 40 min in a 12-well plate. During the experiments, we did not experience any adverse events.

In vitro experiments

BMSP cultures: GLAST^{CreERT2}; Rosa26^{Tom} (Tx P2) or *Wnt-1^{Cre}; Rosa26^{Tom}* mice were euthanized by cervical dislocation or under 5% isoflurane. The femur and tibia were dissected from, and BM was extruded using DMEM low glucose (Gibco) supplemented with 10% FBS. The suspension of BM mononuclear cells (BM-MNCs), at a density of 5×10^5 cells/cm^2, was seeded in 145 mm Petri dishes (Greiner Bio-One). These cultures were incubated with the same cell culture medium, which was changed every 72 h until reaching a 90% confluency. Before the first passage, colonies consisting only of Tom$^+$ cells obtained from *GLAST^{CreERT2}; Rosa26^{Tom}* (Tx P2) or *Wnt-1^{Cre}; Rosa26^{Tom}* mice were identified and marked using a fluorescent microscope (Nikon Eclypse NiE, Melville, NY, USA): the colonies were outlined by drawing a line on the plastic, demarcating the boundaries of the Tom$^+$ colonies. These cultures were then trypsinized using 0.25% trypsin with 1mM EDTA. The Tom$^+$ colonies were lifted, dissociated, and replated at 5×10^3 cells/cm^2 using the same culture medium. Subsequently, Tom$^-$ were lifted and replated separately. This process was repeated for the first 3 passages in cultures with Tom$^+$ cells, leading to cultures enriched in GLAST$^+$ Wnt1$^+$ BMSPs. For both Tom$^+$ and Tom$^-$ cultures, the procedure of trypsinization, lifting, and replating was repeated, after 80–90% confluency, until reaching P8.

Preparation of conditioned media (CM) from BMSP cultures To prepare CM, Tom$^+$ and Tom$^-$ (2×10^4 cells) were separately seeded in 96 mm Petri dishes. On the following day, the cultures were maintained without FBS overnight. Subsequently, the cells were treated with IMT504 or the vehicle for 2 h, followed by a wash and another 22 h of incubation with half the volume of serum-free medium. The culture medium was then centrifuged and the resulting supernatant was aliquoted and frozen until use.

Fibrotic macrophages Macrophages were isolated from CD1 mice that had been previously treated with TAA for a duration of 6 weeks (see above). The cells were incubated for a total of 24 h, consisting of a 2-hour stimulation with IMT504 followed by 22 h with RPMI+2%FBS. The next conditions were set: RPMI+2%FBS (control), RPMI+2%FBS+IMT504 (IMT504 at a concentration of 0.5 µg/ml) or a mixture of 50% v/v CM obtained from Tom$^+$ or Tom$^-$, either pretreated with IMT504 during 2 h followed by 22 h of recovery or untreated. Following the incubation period, the cells were washed and harvested for mRNA expression analysis using qPCR.

Hepatocytes Hepatocytes were derived from the parenchymatic fraction of healthy CD1 mice, as described above. After a 24-hour incubation, these hepatocytes were subjected to an additional 24-hour period of incubation under various conditions. These conditions included DMEM/F12+2%FBS (control), DMEM/F12+2%SFB+IMT504 (incubation with IMT504 for 2 h followed by 22 h in DMEM/F12+2%SFB), or a mixture of 50% v/v CM obtained from Tom$^+$ or Tom$^-$, either pretreated with IMT504 or untreated. After one day, the cells were washed and collected for mRNA expression analysis using qPCR.

Ito cells The CFSC-2G hepatic stellate cell line, originally obtained from cirrhotic rat liver, was kindly provided by Dr. Marcos Rojkind (Albert Einstein College of Medicine, New York, NY, USA). They were cultivated in αMEM supplemented with 10% FBS (Life Technologies, Carlsbad, CA, USA) and non-essential amino acids. To assess the effect of IMT504 and other experimental conditions on these cells´ expression profile, they were incubated with: αMEM+2%SFB (control); αMEM /F12+2%FBS+IMT504 (2 h of incubation followed by 22 h of recovery), or a mixture of 50% v/v CM from Tom$^+$ or Tom$^-$ cells, with or

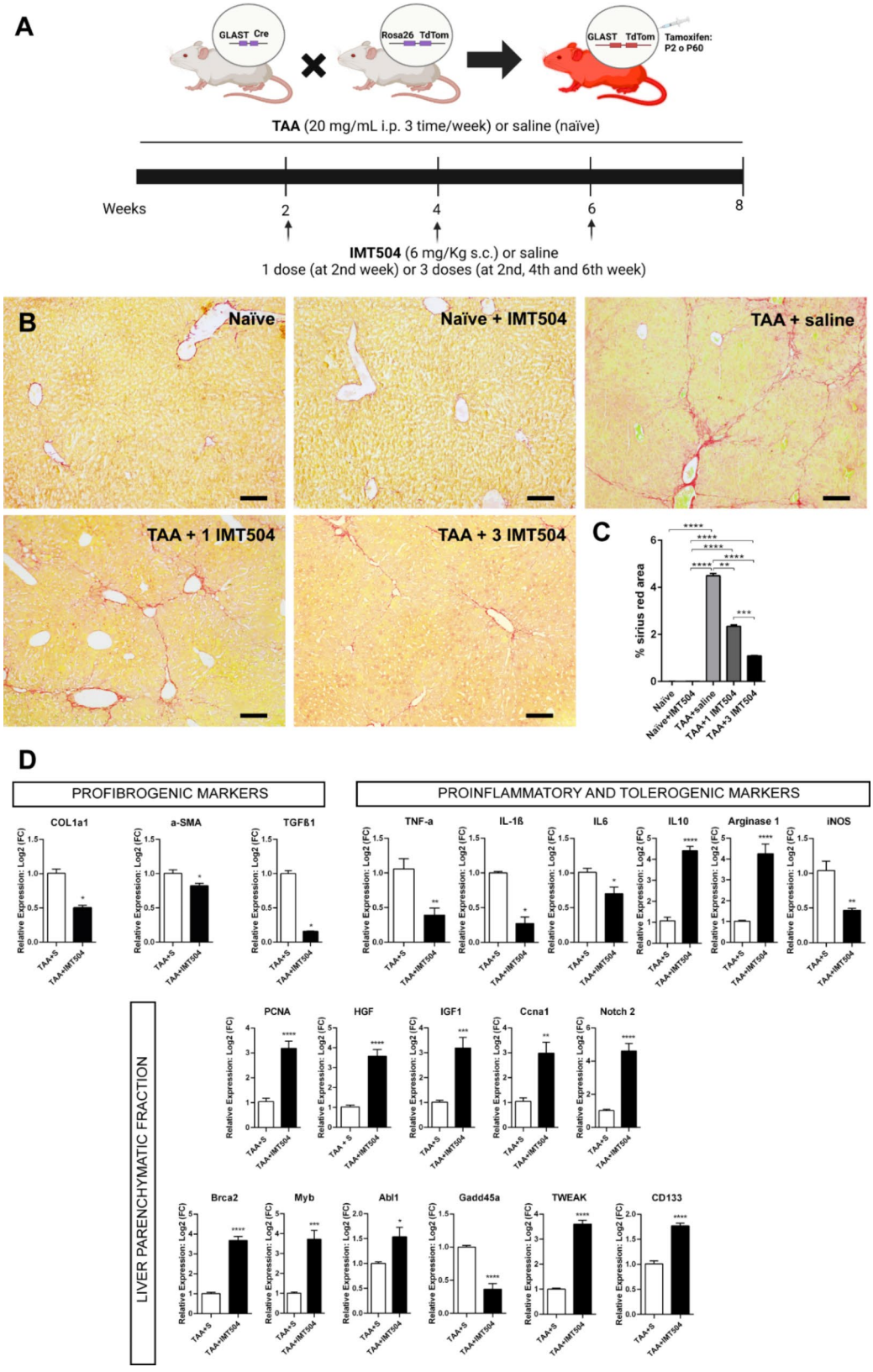

Fig. 1 (See legend on next page.)

(See figure on previous page.)

Fig. 1 IMT504 inhibits liver fibrogenesis. (**A**) Schematic view of derivation of GLAST^{CreERT2};Rosa26^{tdTomato} mice and of the experimental design. (**B**) Representative micrographs showing Sirius red staining of liver sections obtained from *GLAST^{CreERT2}*; *Rosa26^{Tom}* mice (Tx P2) from different experimental groups. Scale bars: 200 µm. (**C**) Statistical comparisons in between groups. **$p < 0.01$; ***$p < 0.001$; ****$p < 0.0001$; Dunn`s multiple comparisons test; $n = 4$. (**D**) Statistical comparisons of qPCR expression levels of profibrogenic and immunomodulatory markers in whole liver tissue, and of proliferation, DNA repair, hepatocyte function and cellular stress in the parenchymatic-enriched liver fraction at 1 day after IMT504 or vehicle-application, 2 weeks after TAA-treatment onset. *$p < 0.05$; **$p < 0.01$; ***$p < 0.001$; ****$p < 0.0001$; *vs. TAA + S. Mann-Whitney: COL1a1, a-SMA, TGF-β1, IL-1β and iNOS; unpaired t-student: all other markers

without prior IMT504 treatment. Subsequently, the cells were washed and collected for mRNA expression analysis.

Proliferation assay and flow cytometry

P8 Tom$^+$ or Tom$^-$ BMSPs were plated in 96 mm petri dishes. Upon reaching 80% confluency, the cells were or not subjected to a 2-hour treatment with IMT504 (0.5 µg/ml). Some cells were incubated with CHIR (9 µM), known to elicit Wnt signaling and nuclear translocation of beta-catenin [24], Dkk1 (200 ng/ml; R&D; Wnt antagonist), or a combination of IMT504 and Dkk1 or IMT504 and IWR1 (10 µM; Sigma-Aldrich; Wnt1 inhibitor) [25, 26]. Afterward, the culture media was replaced to eliminate IMT504 and/or factors activating/inhibiting Wnt signaling. Four hours later, cells from various conditions were detached and fixed using 4% paraformaldehyde for subsequent flow cytometry analyses involving Ki67 immunolabeling. The cells were washed thrice with FACS buffer (1xPBS-1% BSA) through centrifugation (5 min at 1000 rpm) and resuspension. Following this, the cells were transferred to flow cytometry tubes (10^6 cells per tube) and incubated for 45 min with an unconjugated polyclonal rabbit anti-Ki67 primary antibody (1/100; abcam ab15580) along with FACS buffer and 0.1% saponin, for 45 min, all in darkness. After two additional rounds of washing with FACS buffer, the cells were incubated with 100 µl AlexaFluor 488®- or AlexaFluor 594®-coupled secondary antibodies (Invitrogen, Thermo Fisher Scientific, Waltham, MA, USA) at a 1/100 dilution in FACS buffer and 0.1% saponin for 45 min. After two more washing, the cells were fixed again with paraformaldehyde and maintained in 100 µl of 1xPBS until flow-cytometry analysis. Other markers used in flow cytometry experiments were: mouse monoclonal anti-Albumin (Santa Cruz Biotechnology; sc-374670), rat monoclonal anti-CD31 (BD Pharmingen; 553370), rat monoclonal anti-CD44-APC antibody (BD Pharmingen; 559250) rabbit polyclonal anti-CD133 (Abcam; ab19898), goat anti-Ep-CAM (Santa Cruz Biotechnology; sc-23788). Samples without incubation with primary antibodies were included as control. Flow cytometry analyses were conducted using a Becton–Dickinson FACSAria Fusion, and FlowJo v10.0.8 software (FlowJo, Ashland, OR, USA) was used for data analysis.

Boyden chamber motility assay

In this assay, a standard 48-well microchemotaxis Boyden chamber (Neuro Probe; Cabin John, MD) was utilized. P8 Tom$^+$ or Tom$^-$ BMSPs were cultured in 96 mm Petri dishes until they reached 80% confluency. Subsequently, some dishes were subjected to a 2-hour incubation with IMT504 (0.5 µg/ml), while others were treated with the vehicle. Following a 4-hour recovery period, these cells were seeded at a density of $1{,}2 \times 10^3$ cells/well in the upper chamber of the transwell unit. In the lower chamber either 26 µL of DMEM low glucose or CM obtained from LX-2 cells (a human hepatic stellate cell line) was added. The cells were allowed to migrate from the upper side of the membrane to the lower through 8 µm pores over a period of 4 h at 37 °C. Following this migration period, the membrane was fixed in 4% paraformaldehyde, and the cells that had successfully migrated to the lower side were stained with DAPI (1 mg/ml). A total of three photographs were taken from each replicate using a Zeiss LSM700 fluorescent microscope and total number of cells were counted.

Statistical analysis

Unless explicitly indicated, each experiment was conducted a minimum of two times, with a sample size of at least 4. This sample size allows for obtaining significant differences in statistical comparisons when they are greater than 30%. Values from different experiments were included in the same analysis. All values are presented as mean ± standard error of the mean. Appropriate statistical methods were employed based on the number of groups being compared in each experiment and the distribution characteristics of the data. To determine if the data distribution followed a normal distribution, the Kolmogorov-Smirnov test was applied. A significance level of $p < 0.05$ was deemed as statistically significant. Data analyses was performed using Prism software (GraphPad, San Diego, CA, USA). No data were excluded.

Other specifications can be found in the Supplemental Information.

Results

IMT504 inhibits the progression of fibrogenesis in mice

Considering the immunomodulatory properties of IMT504, we wonder if this ODN could inhibit the progression of liver fibrogenesis. We first verified that TAA treatment led to established fibrosis in *GLAST^{CreERT2}*;

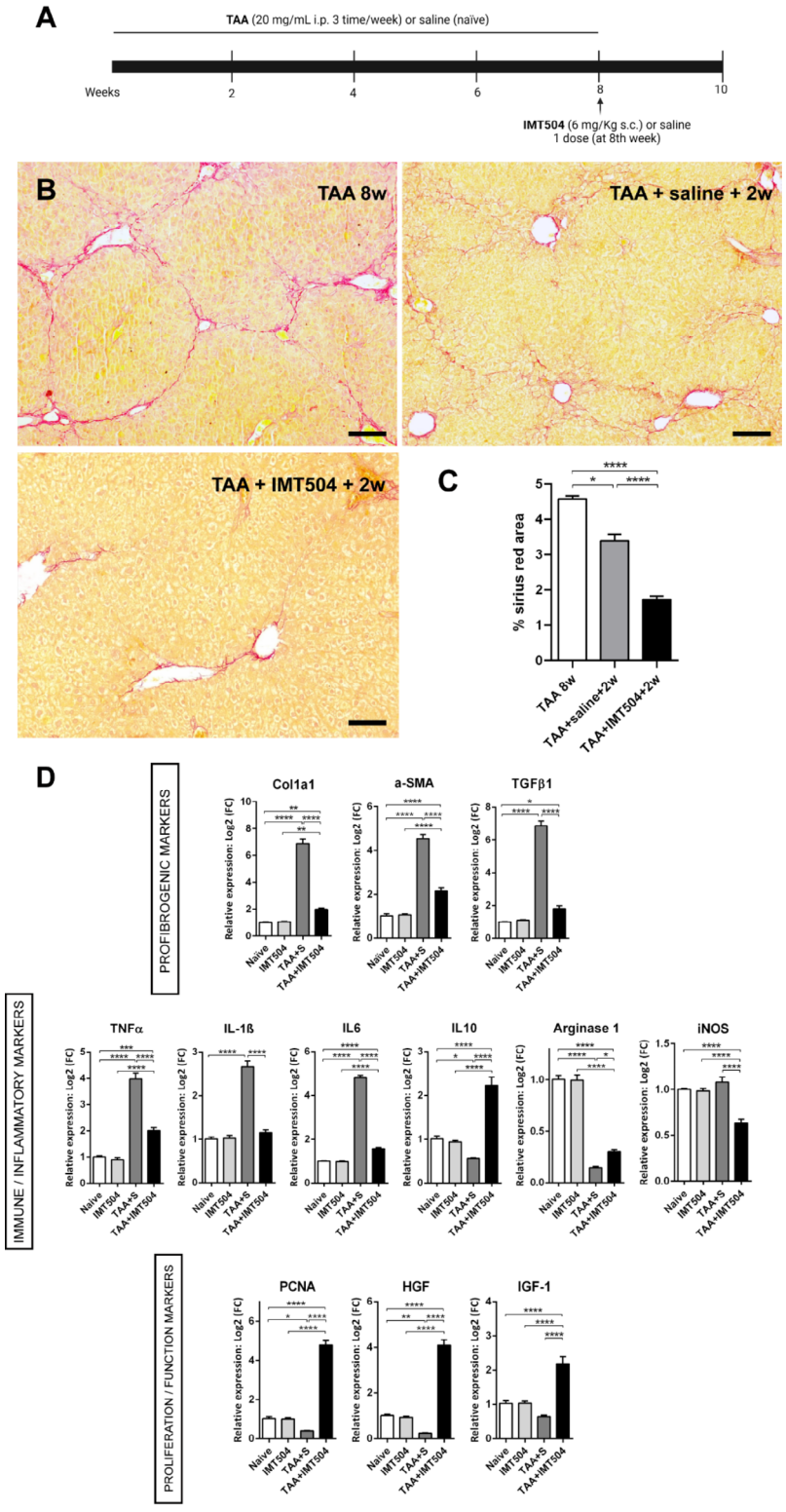

Fig. 2 IMT504 improves regression of liver fibrosis. (**A**) Schematic of the experimental design. (**B**) Representative micrographs showing Sirius red staining of liver sections obtained from CD1 mice of different experimental groups. Scale bars: 200 µm. (**C**) Statistical comparisons in between groups. *$p < 0.05$; ****$p < 0.0001$; Dunn`s multiple comparisons test; $n = 4$. (**D**) Statistical comparisons of qPCR expression levels of profibrogenic, immune/inflammation and proliferation/parenchymal function markers in whole liver tissue at 14 days after saline/IMT504 application (regression model). *$p < 0.05$; **$p < 0.01$; ***$p < 0.001$; ****$p < 0.0001$; Tukey´s multiple comparisons test; $n = 3$

Rosa26^{Tom} (Tx P2) mice after 8 weeks (Fig. 1A). This was assessed by measuring the percentage of Sirius red stained area and quantifying the area of α-smooth muscle actin immunoreactivity. Mice administered a single dose of IMT504, 2 weeks after TAA treatment onset, exhibited a significant reduction in fibrosis degree compared to the control group (Fig. 1B, C; Figure S1). This effect was even more pronounced when mice received 3 doses of IMT504, administered with a 2 week-interval between each dose (Fig. 1B, C; Figure S1). A proinflammatory liver microenvironment, typically associated with the activation of hepatic stellate cells, hinders liver regeneration and hepatocyte proliferation [11]. Supporting the notion that IMT504 plays an immunomodulatory role, an increase in hepatocyte proliferation was found, in relation with the number of IMT504 doses administered (Figure S2).

To delve into the early mechanisms triggered by IMT504 in the liver, wild-type littermates of *GLAST*^{CreERT2}; *Rosa26*^{Tom} (Tx P2) mice were treated with TAA for 2 weeks. These mice were subsequently injected with IMT504 (or vehicle) and were sacrificed after 1 day. Ample material from both the entire liver and parenchymatic fractions were collected, which were then processed for qPCR. IMT504 treatment exhibited a significant reduction in mRNA expression levels of profibrogenic markers (col1a1, α-SMA and TGF-β1) as well as pro-inflammatory markers (TNF-α, IL-1β, IL-6 and iNOS) (Fig. 1D). Furthermore, it led to an increase in tolerogenic markers (IL-10 and Arginase-1). Additionally, within the parenchymatic fraction, an upregulation of markers associated with hepatoblast/hepatocyte proliferation (HGF, PCNA, Notch2), hepatocyte function (IGF-I), DNA synthesis and repair quality control (Brca2, Myb, Abl1), and positive regulation of cell-cycle progression (Ccna1) was found. Conversely, the expression levels of Gadd45α (a marker of cellular stress, DNA damage and cell cycle arrest) were found to be downregulated. Interestingly, two markers of liver progenitor cells, TWEAK (TNF-like weak inducer of apoptosis) and CD133 [28, 29], were found to be overexpressed in the liver parenchymatic fraction of animals treated with the ODN.

To ascertain whether IMT504 could alleviate liver fibrosis in a different in vivo model with a distinct etiology, CD1 mice were subjected to bile-duct ligation (BDL). Five days after BDL, these mice were administered IMT504 or saline and were euthanized 9 days later. IMT504 treatment was associated with reduced collagen fiber deposits and myofibroblast activation, while also stimulating hepatocyte proliferation (Figure S3). Consequently, these findings confirm the ability of IMT504 to ameliorate liver fibrosis in different in vivo mouse models.

IMT504 facilitates liver fibrosis regression in mouse TAA model

We subsequently investigated whether IMT504 could also facilitate the regression of pre-existing fibrosis. To address this, a single dose of IMT504 or vehicle was administered to wild-type littermates of *GLAST*^{CreERT2}; *Rosa26*^{Tom} (Tx P2) mice after a 8-week TAA treatment (Fig. 2A). Following this intervention, the animals underwent a two-week recovery period without further TAA applications. After this period, the mice were humanely euthanized, and their livers were extracted and processed for analysis.

The administration of IMT504 significantly improved fibrosis regression: it led to a substantial reduction in both the Sirius Red stained-area (Fig. 2) and the area immunostained for α-smooth muscle actin, a marker of myofibroblast activation (Figure S4). Additionally, there was a significantly increase in the number of PCNA$^+$ hepatocytes, indicating enhanced proliferation, in the IMT504-treated group (Figure S4). Furthermore, our analysis of mRNA expression levels at the end of the experiment revealed promising findings (Fig. 2). When compared to the vehicle control, IMT504 condition resulted in significant reductions of profibrogenic and proinflammatory markers. Some of them, such as TGF-β1 and IL-1β, even return to normal levels. Notably, IL-10 expression remained significantly upregulated, while iNOS expression was downregulated compared to control groups, including naïve mice. Hepatocyte proliferation and functional markers were also upregulated. Collectively, these data support the conclusion that IMT504 accelerates recovery from liver fibrosis.

To investigate the early mechanisms underlying IMT504-mediated acceleration of liver fibrosis regression, we conducted new analyses. Animals treated with TAA for 8 weeks were sacrificed 24 h after the application of IMT504, and their liver samples were processed for qPCR analysis. The results closely resembled those obtained when IMT504 was administered at 2 weeks of TAA treatment, specifically concerning profibrogenic, proinflammatory, hepatocyte proliferation, and hepatocyte progenitor markers (Figure S4).

IMT504 likely enhances the contribution of GLAST+ Wnt1+ BMSPs with endothelial-like cells and hepatocyte-like cells during liver fibrogenesis

Previously, we demonstrated that GLAST$^+$ Wnt1$^+$ BMSPs, a subpopulation of perisinusoidal stromal cells, become mobilized to the peripheral blood and may contribute to ELCs and HLCs following liver injury [9]. Given that IMT504 is known to induce the mobilization of BMSPs into the bloodstream [16], we sought to determine whether this ODN could also enhance the

contribution of the subpopulation of GLAST$^+$ Wnt1$^+$ BMSPs to liver cells during fibrogenesis.

To address this, we crossed *GLAST^{CreERT2}* with *Rosa26^{Tom}* heterozygous mice (Fig. 1A). The resulting double-transgenic offspring enable the identification of GLAST$^+$ cells at the moment of tamoxifen (Tx) injection through the expression of the tdTomato (Tom) reporter gene. This allows us to identify GLAST$^+$ Wnt1$^+$ BMSPs in the bone marrow or, if mobilized through the bloodstream, in the organs where they are recruited, and to determine the cell types they give rise to. Adult *GLAST-^{CreERT2}*; *Rosa26^{Tom}* mice (Tx postnatal day -P-2) were injected intraperitoneally (i.p.) with TAA for 8 weeks. Consistent with our hypothesis, animals that received a single dose of IMT504 at the second week of TAA treatment exhibited a higher incidence of Tom$^+$ ELCs (Fig. 3; Movies S1 and S2) and HLCs (Fig. 4) compared to the vehicle control group. Moreover, this effect was significantly more pronounced in animals receiving three doses of IMT504 -administered at the 2nd, 4th and 6th weeks of TAA treatment- (Figs. 3 and 4; Movie S3). Interestingly, IMT504 was also found to promote the proliferation of GLAST-traced ELCs and HLCs in the liver after 8 weeks of TAA treatment (Figs. 3 and 4).

We then investigated whether GLAST$^+$ Wnt1$^+$ BMSPs can acquire the expression of ELC and HLC specific markers both in vitro and in vivo. To achieve this, we cultured a fraction enriched in this BMSP subpopulation for 7 days with conditioned media from hepatectomized liver, which led to the acquisition of ELC and HLC specific markers (Figure S5). Additionally, we injected the bone marrow mononuclear fraction obtained from *Wnt-1^{Cre}*; *Rosa26^{Tom}* mice into athymic mice that had undergone hepatectomy 5 days prior. Five days post-transplant, flow cytometry analysis revealed that a fraction of Tom$^+$ cells coexpressing CD44 and fibronectin had acquired ELC (Figure S6) and HLC specific markers (Figure S7). This suggests that GLAST$^+$ Wnt1$^+$ BMSPs may have the potential to differentiate into both ELCs and HLCs.

In addition, we found that CD44$^+$ Tom$^+$ cells in the bone marrow and peripheral blood coexpress CD133, a well-known progenitor marker (Figure S8A, B). CD133 is also a liver progenitor marker in cells that coexpress albumin [28]. Therefore, our data may suggest that GLAST$^+$ Wnt1$^+$ BMSPs are likely to acquire ELC and HLCs specific markers and contribute to liver progenitors. Given the possibility that some GLAST$^+$ endothelial and/or hepatocyte progenitors may reside in the liver, we analyzed the incidence of CD31$^+$ Tom$^+$ cells, and the coexpression of CD133 and albumin in Tom$^+$ cells, by flow cytometry. Virtually no Tom$^+$ ELCs were found in the liver of naïve or IMT504-treated double-transgenic mice injected with tamoxifen at P60 (Figure S8F). And with regards to the liver parenchymatic fraction, in some, but not all, naïve and IMT504-treated *GLAST^{CreERT2}*; *Rosa26^{Tom}* (TxP2) mice a minor fraction of CD133$^+$ Albumin$^+$ Tom$^+$ cells was found (0.012±0.0169% and 0.0237±0.0336%; naïve and IMT504, respectively; of total parenchymatic cells). A similar pattern was observed when CRE recombination (Tom expression) was induced at P60, although the incidence of CD133$^+$ Albumin$^+$ Tom$^+$ was reduced (0.0004±0.0008% and 0.0011±0.0001%; naïve vs. IMT504) (Figure S8C, G). In contrast, significantly higher numbers of CD31$^+$ Tom$^+$ ELCs and CD133$^+$/Ep-CAM$^+$ Albumin$^+$ Tom$^+$ HLCs were observed in the liver of all TxP2- and Tx P60-injected mice treated with TAA and IMT504 (Figure S8C, G). Overall, these findings suggest that although some GLAST$^+$ liver progenitors may eventually exist in the liver, non-resident Tom$^+$ cells (likely GLAST$^+$ Wnt1$^+$ BMSPs) give rise to Tom$^+$ ELCs, HLCs and liver progenitors following injury, with IMT504 expanding these subpopulations.

IMT504 enhances the incidence within the bone marrow of GLAST+ Wnt1+ BMSPs in the context of fibrosis

Previously, we demonstrated that TAA reduces the capacity of GLAST$^+$ Wnt1$^+$ BMSPs to form dense colonies in a colony-forming unit assay during early liver fibrogenesis [9]. We asked whether IMT504 treatment could expand the GLAST$^+$ Wnt1$^+$ BMSPs pool and ultimately restore their ability to form dense colonies again. This could partially explain the increased contribution of GLAST$^+$ Wnt1$^+$ BMSP-derived cells to liver regeneration mediated by IMT504. To address this, we systemically administered IMT504 to *Wnt1^{Cre}*; *Rosa26^{Tom}* mice previously treated with TAA during 2 weeks. Eighteen hours later, we performed a colony-forming unit-fibroblasts (CFU-Fs) assay using the BM-MNCs fraction. A significant increased incidence of Tom$^+$ CFU-Fs was observed in the IMT504-treated group compared to the naïve control (Fig. 5A, B). Similarly, when IMT504 was applied to TAA-treated mice, the number of Tom$^+$ CFU-Fs increased compared to TAA-treated animals receiving a vehicle injection (Fig. 5A, B). Interestingly, the increase in CFU-Fs induced by IMT504 was only seen in the Tom$^+$ BMSP subpopulation (Fig. 5A, B). Notably, IMT504 was found to restore the capacity of GLAST$^+$ Wnt1$^+$ BMSPs to form dense colonies (Fig. 5C).

As Wnt signaling is frequently associated with proliferation and mobilization of progenitor cells [30–33], we sought to determine whether IMT504 could de novo activate Wnt1 in Tom$^-$ stromal progenitor cells. BM-MNCs from *Wnt1^{Cre}*; *Rosa26^{Tom}* mice were plated in 6 well-plates and Tom$^+$ and Tom$^-$ colonies were quantified once colonies formed (control, 0 h). Subsequently, these cultures were incubated with IMT504 for 2 h, and the percentage of colonies was re-quantified 24 and 48 h later.

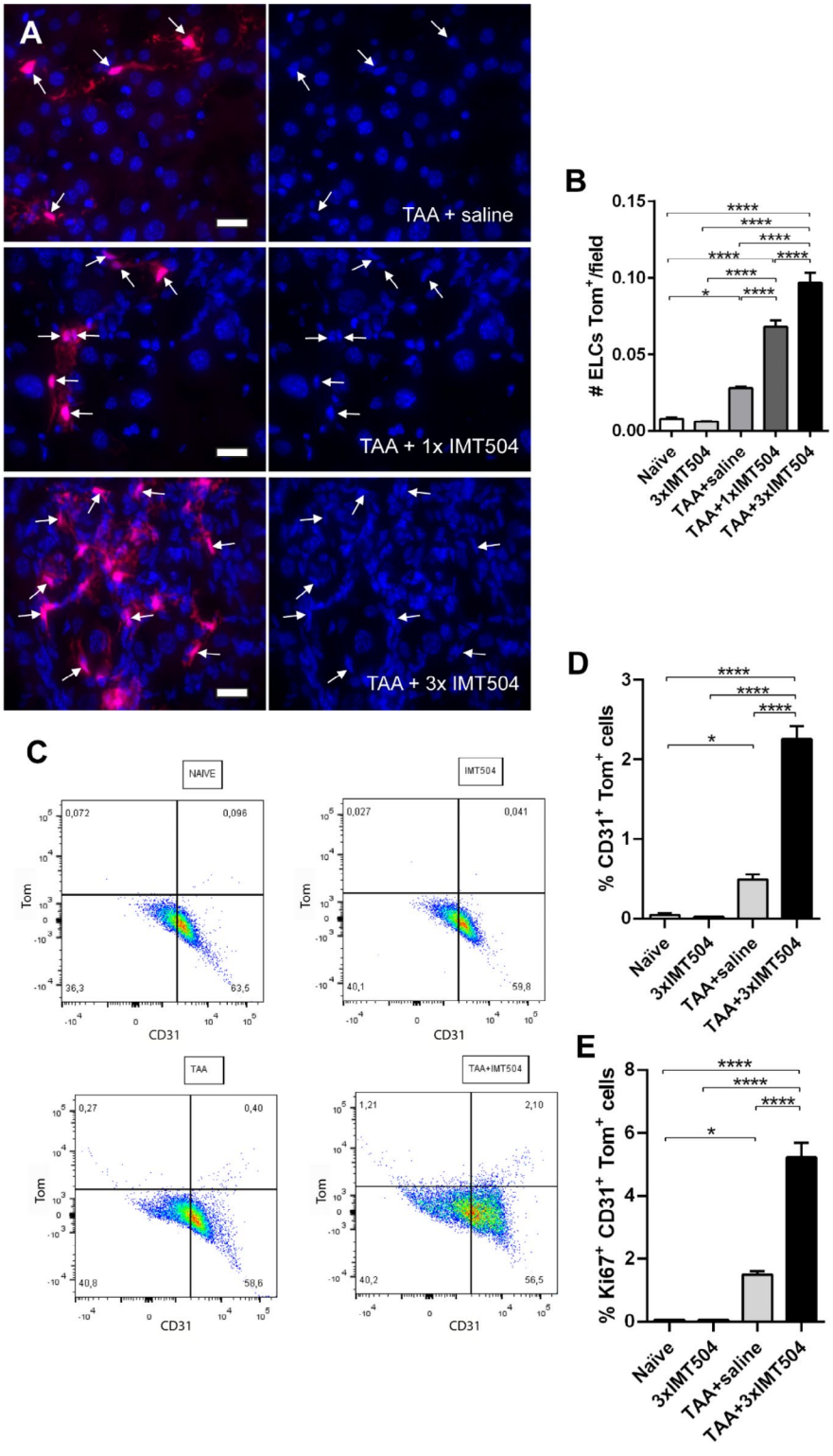

Fig. 3 IMT504 likely enhances the contribution of GLAST^{+} Wnt1^{+} BMSPs with ELCs in the liver during fibrogenesis. (**A**) Representative microphotographs showing ELCs Tom^{+} in *GLAST^{CreERT2}*; *Rosa26^{Tom}* mice (Tx P2) of different experimental groups. Scale bars: 20 µm. (**B**) Statistical comparisons of numbers of endothelial-like Tom^{+} cells; $n=4$. (**C**) Representative flow cytometry plots showing the abundance of CD31^{+} Tom^{+} in the non-parenchyma enriched fraction of the liver. (**D**) Statistical comparisons of percentage of CD31^{+} Tom^{+} ELCs, in the non-parenchymatic liver fraction, from flow cytometry analyses; $n=5$. (**E**) Statistical comparisons of percentage of Ki67^{+} cells among the total of CD31^{+} Tom^{+} ELCs, from flow cytometry analyses; $n=4$. (**B, D,E**) *$p<0.05$; **$p<0.01$; ****$p<0.0001$. Tukey`s multiple comparisons test

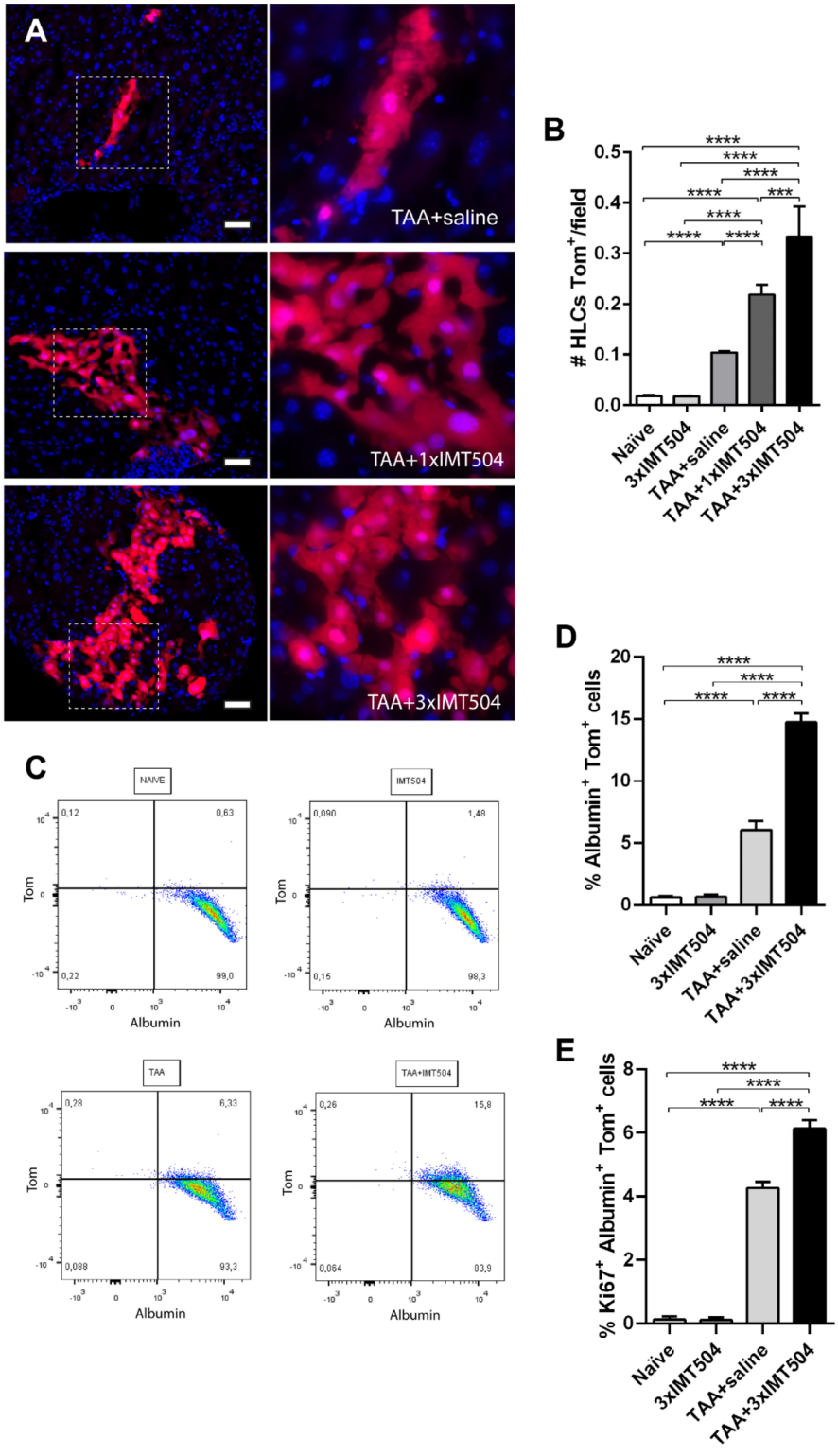

Fig. 4 IMT504 likely enhances the contribution of GLAST$^+$ Wnt1$^+$ BMSPs with HLCs in the liver during fibrogenesis. (**A**) Representative microphotographs showing Tom$^+$ HLCs in *GLAST^{CreERT2}*; *Rosa26^{Tom}* mice (Tx P2) of different treatments. Scale bars: 20 µm. (**B**) Statistical comparisons of numbers of Tom$^+$ HLCs; $n=4$. (**C**) Representative flow cytometry plots showing the abundance of Albumin$^+$ Tom$^+$ in the parenchyma enriched fraction of the liver. (**D**) Statistical comparisons of the percentage of Albumin$^+$ Tom$^+$ HLCs, from flow cytometry analyses; $n=4$. (**E**) Statistical comparisons of percentage of Ki67$^+$ cells among the total of Albumin$^+$ Tom$^+$ HLCs, from flow cytometry analyses; $n=4$. (**B, D, E**) ***$p<0.001$; ****$p<0.0001$; Tukey`s multiple comparison test

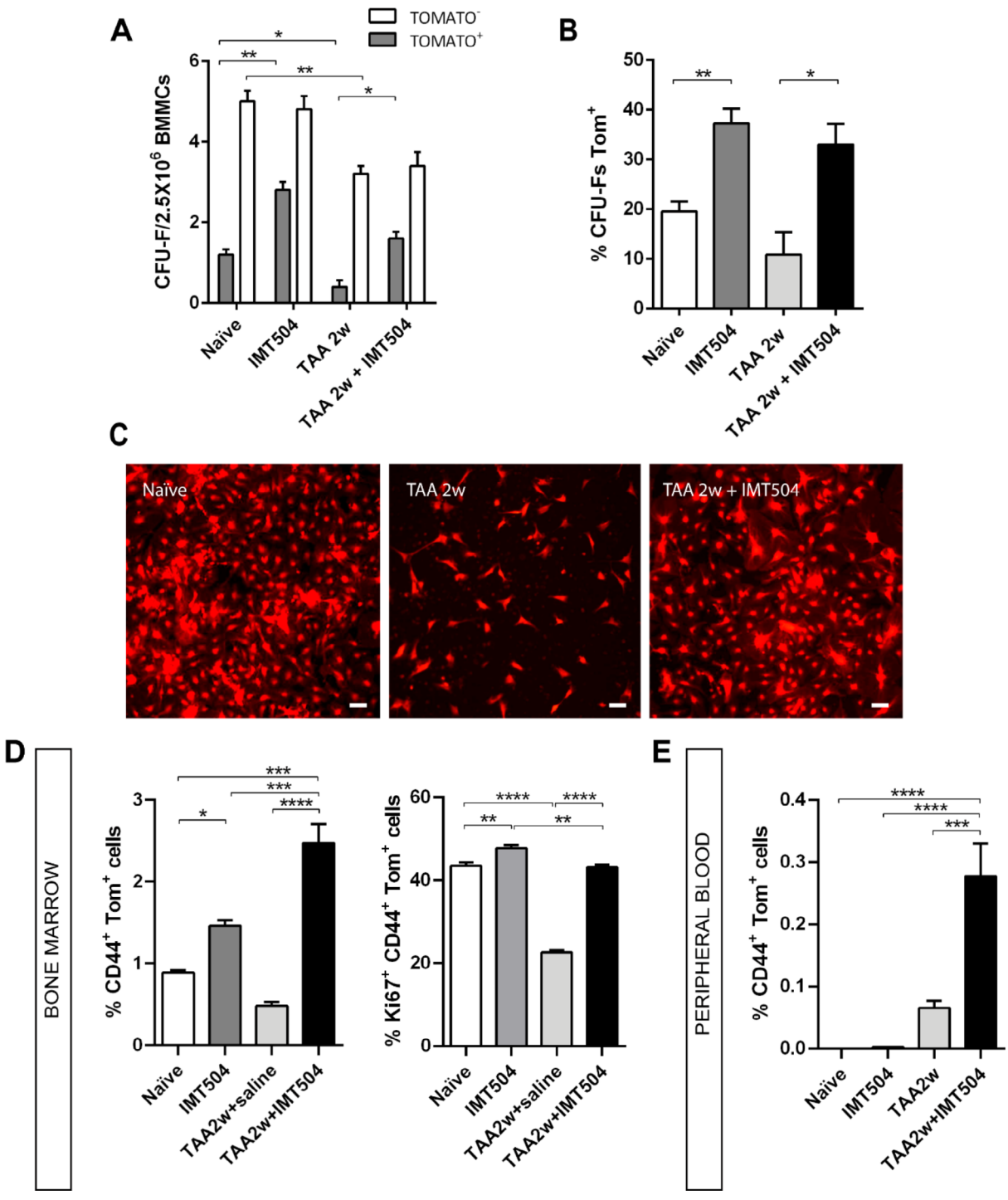

Fig. 5 In vivo effect of IMT504 on Wnt1 or GLAST-traced bone marrow mononuclear cells. (**A**) Statistical comparisons of numbers of CFU-Fs, Tom^+ or Tom^-, obtained from BM-MNCs of *Wnt1*^{Cre}; *Rosa26*^{Tom} which were or not treated with TAA during 2 weeks, and were s.c. injected or not with IMT504. (**B**) Statistical comparisons of percentage of CFU-Fs Tom^+. (**A, B**) Dunn`s multiple comparison test; $n=6$. (**C**) Microphotographs showing representative colonies obtained from naïve, TAA 2w and TAA 2w + IMT504 treated mice. Scale bar: 50 µm. (**D**, left) Statistical comparisons of percentage of $CD44^+$ Tom^+ cells within the bone marrow after 2 weeks of TAA and/or IMT504 treatments, as measured by flow cytometry. (**D**, right) Statistical comparisons of percentage of $Ki67^+$ cells among the total of $CD44^+$ Tom^+ cells within the bone marrow from *GLAST*^{CreERT2}; *Rosa26*^{Tom} (Tx P2) after 2 weeks of TAA and IMT504/saline treatments, as measured by flow cytometry. (**E**) Statistical comparisons of percentage of $CD44^+$ Tom^+ cells within the peripheral blood after 2 weeks of TAA and IMT504/saline treatments, as measured by flow cytometry. (**D, E**) Turkey`s multiple comparison test; $n=4$. (**A, B,D, E**) $^*p<0.05$; $^{**}p<0.01$; $^{***}p<0.001$; $^{****}p<0.0001$

As shown in Figure S9, there were no significant changes in the proportion of Tom^+ colonies. From this result, we conclude that IMT504 is unlikely to induce *de novo* activation of the Wnt1 promoter in previously Tom^- BMSPs.

We then analyzed the incidence of $GLAST^+$ $Wnt1^+$ BMSPs in the BM and peripheral blood of $GLAST^{CreERT2}$; $Rosa26^{Tom}$ mice (Tx P2 or P60) treated with TAA during 2 weeks and injected with IMT504 or vehicle 24 h before, by flow cytometry. As expected, the frequency of $CD44^+$ Tom^+ cells notably rose in the bone marrow after IMT504 treatment (Fig. 5D, left; Figure S8D; Figure S10A). Furthermore, liver injury prompted the mobilization of $GLAST^+$ $Wnt1^+$ BMSPs toward the peripheral blood, a phenomenon significantly potentiated by IMT504 (Fig. 5E; Figure S8E). Hence, IMT504 appears to stimulate both the expansion and mobilization of $GLAST^+$ $Wnt1^+$ BMSPs in vivo. Similar results were found in bone marrow and peripheral blood samples obtained from mice treated with TAA during 8 weeks and three doses of IMT504 (Figure S11).

In summary, these results suggest that IMT504 induces the expansion of $GLAST^+$ $Wnt1^+$ BMSPs and restores their capacity to form dense colonies in the context of TAA-mediated early fibrogenesis. These findings lead us to conclude that IMT504 can promote the expansion of $GLAST^+$ $Wnt1^+$ BMSPs in vivo, likely contributing to the increase incidence of Tom^+ ELCs and HLCs during liver fibrogenesis.

IMT504 stimulates the proliferation of GLAST + Wnt1 + BMSPs with the induction of Wnt signaling pathway

To assess whether IMT504 could stimulate the proliferation of $GLAST^+$ $Wnt1^+$ BMSPs in vivo, we conducted flow cytometry analyses and quantified the percentage of $GLAST^+$ $Wnt1^+$ BMSPs expressing Ki67 in the BM of $GLAST^{CreERT2}$; $Rosa26^{Tom}$ mice (Tx P2) treated with or without TAA over a 2-week period, followed by euthanasia one day after the administration of a single dose of IMT504 or vehicle. IMT504 was able to augment the proportion of $GLAST^+$ $Wnt1^+$ BMSPs when applied to naïve mice (Fig. 5D, right). As anticipated, TAA treatment diminished the proliferative capacity of $GLAST^+$ $Wnt1^+$ BMSPs, a phenotype which was rescued by IMT504 (Fig. 5D, right; Figure S10B). Additionally, at one day post-treatment, IMT504 not only increased the abundance of $CD31^+$ Tom^+ ELCs following 2 weeks of TAA treatment (Figure S10C), but also augmented the proportion of $Ki67^+$ proliferating Tom^+ cells within the $CD31^+$ cell population (Figure S10D). These features were also found in the fraction of $Albumin^+$ Tom^+ HLCs (Figure S10E, F). These findings corroborate the data presented in Figs. 3 and 4, suggesting that increased proliferation of Tom^+ ELCs and Tom^+ HLCs occur shortly after the application of the oligodeoxynucleotide.

To further confirm the role of IMT504 in promoting the proliferation of $GLAST^+$ $Wnt1^+$ BMSPs, we established primary cultures from $GLAST^{CreERT2}$; $Rosa26^{Tom}$ BM-MNCs and separately expanded fractions enriched in Tom^+ and Tom^- cells, allowing them to reach at least 10 passages (P10) in vitro. By P7, 79.97 ± 1.29% of cells in the Tom^+ cultures expressed the reporter gene, whereas virtually no Tom^+ cells were detected in Tom^- cultures (not shown). To assess the impact of IMT504 on the proliferation of P8 $GLAST^+$ $Wnt1^+$ BMSPs, Tom^+ and Tom^- fractions were pretreated with IMT504 for 2 h. After 4 h, flow cytometry analysis revealed a significantly increase in $Ki67^+$ proliferating BMSPs, rising from ~ 30% to ~ 75%, exclusively in the Tom^+ cells incubated with IMT504 (Fig. 6A, B). This was confirmed in P8 $GLAST^+$ $Wnt1^+$ BMSPs derived from $Wnt1^{Cre}$; $Rosa26^{Tom}$ mice (Fig. 6B).

Given our ability to trace $GLAST^+$ $Wnt1^+$ BMSPs owing to their early expression of Wnt1, and considering that Wnt signaling is known to induce the proliferation and mobilization of various progenitors, we then asked whether $GLAST^+$ $Wnt1^+$ BMSPs express Wnt1 and Wnt signaling pathway or target markers in the adult. Semi-confluent P8 Tom^+ and Tom^- cells were deprived from serum during 22–40 h, and samples were processed for qPCR analysis. Notably, mRNA expression levels of Wnt1, β-catenin and the canonical Wnt signaling target gene Cyclin-D1 [34] were higher in Tom^+ compared to Tom^- BMSPs (Fig. 6C). Moreover, their expression levels further increased in Tom^+ cells when subjected to longer incubation times in serum-deprived conditions, whereas they remained unchanged in Tom^- cells.

Since Wnt1 signaling pathway is specifically active in $GLAST^+$ $Wnt1^+$ BMSPs, we asked whether Wnt signaling might be modulated by IMT504 in these progenitors. To explore this, P8 Tom^+ and Tom^- cells were incubated with IMT504 or with vehicle for 2 h, and were allowed to recover for 4–22 h in a serum deficient culture medium. Subsequently, samples were collected and processed for qPCR analysis. While Wnt1 mRNA expression levels remained unchanged in Tom^- cells, a 400x increase in this marker was observed in Tom^+ cells after 2 + 4 h, and it was further upregulated in the 2 + 22 h IMT504-treatment condition (Fig. 6D). Similar patterns were observed for beta-catenin and Cyclin-D1. Additionally, other genes positively regulated by Wnt, including Axin2, Lef1 and Sp5, exhibited similar patterns of overexpression, along with a minor although significant increase in the ligand Wnt3a (Figure S12).

To analyze whether Wnt signaling is involved in the observed induction of $GLAST^+$ $Wnt1^+$ BMSPs proliferation by IMT504, we treated these cells with IMT504 and either Dkk1 (a Wnt antagonist) or IWR1 (a Wnt

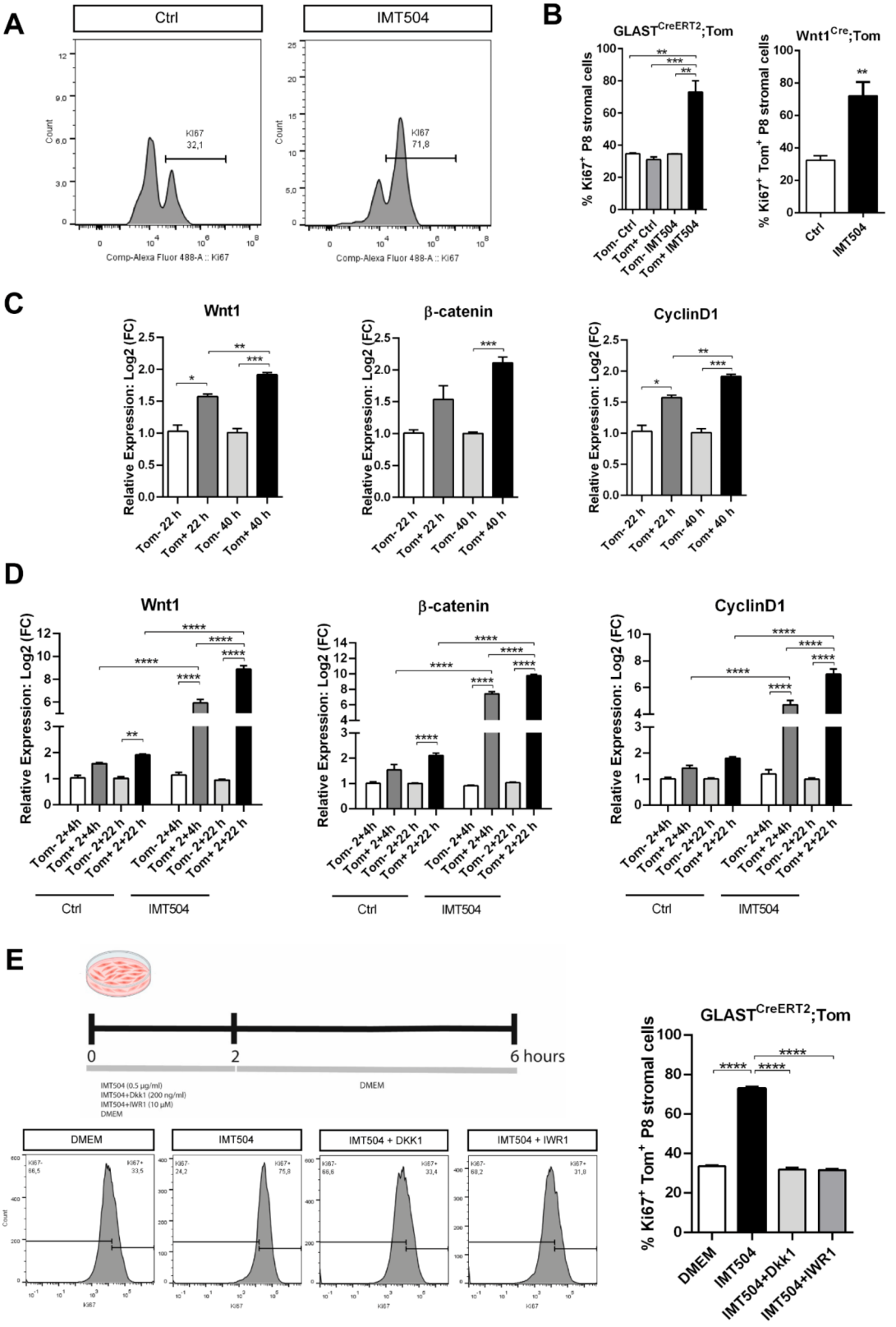

Fig. 6 (See legend on next page.)

(See figure on previous page.)

Fig. 6 Effect of IMT504 on the proliferation of P8 GLAST$^+$ Wnt1$^+$ BMSPs (**A**) Representative histograms from flow-cytometry analyses of Tom$^+$ cells, treated or not with IMT504, immunolabeled for Ki67, and (**B**) statistical comparisons in between Tom$^+$ and/or Tom$^-$ cells of different experimental conditions obtained from different double-transgenic mice; left, Tukey´s multiple comparisons test ($n=6$); right: t-student ($n=5$). (**C**) Statistical comparisons showing changes in Wnt1, β-catenin and Cyclin-D1 mRNA expression levels, obtained by qPCR analyses, in between vehicle-treated Tom$^+$ and Tom$^-$ cells. (**D**) Statistical comparisons showing changes in Wnt1, β-catenin and Cyclin-D1 expression levels, obtained by qPCR analyses, in between cells which were treated with vehicle (Ctrl) or IMT504. (**E**) Experimental schematic figure, representative histograms from flow-cytometry analyses of Tom$^+$ cells immunolabeled for Ki67 and statistical comparisons in between different experimental conditions. (**C-E**) Tukey´s multiple comparisons test; $n=4$. (**B-E**) *$p<0.05$; **$p<0.01$; ***$p<0,001$; ****$p<0.0001$

inhibitor). This treatment blocked the proliferative effect of IMT504 (Fig. 6E). Furthermore, the ability of IMT504 to induce Wnt signaling in GLAST$^+$ Wnt1$^+$ BMSPs was confirmed by incubating the cells with CHIR, a specific Wnt activator (57.83±2.8 vs. 33.41±1,19; CHIR vs. DMEM; $p<0.0001$; $n=3$; t-student test). In conclusion, our results suggest that IMT504 stimulates the proliferation of GLAST+Wnt1+BMSPs likely through the induction of the Wnt signaling pathway.

IMT504 promotes the mobilization of in vitro expanded GLAST+Wnt1+BMSPs

To determine if IMT504 could enhance the motility of P8 GLAST$^+$ Wnt1$^+$ BMSPs, we conducted an in vitro Boyden chamber assay. As expected, IMT504-treated Tom$^+$ cells exhibited the highest motility score (Fig. 7). Interestingly, when GLAST$^+$ Wnt1$^+$ BMSPs were treated with IMT504, they displayed the ability to migrate even in the absence of chemoattractants to the same extent as Tom$^-$ cells in the presence of conditioned media from LX2 cells, a condition known to induce the migration of stromal progenitor cells [35]. Furthermore, Tom$^+$ cells displayed an overall higher motility capacity compared to Tom$^-$ with the latter showing limited mobilization ability.

It is well established that Wnt canonical signaling pathway can influence cell motility by downregulating E-cadherin expression levels [36]. In line with this, incubating P8 GLAST+Wnt1+BMSPs with IMT504 and allowing them to recover for 4 h resulted in reduced E-cadherin mRNA expression levels compared to control Tom$^+$ cells. These levels were further reduced when Tom$^+$ cells were collected 22 h after IMT504 stimulation (Fig. 7C). In contrast, no significant changes were observed in Tom$^-$ cells, whether or not they received IMT504 treatment. Interestingly, control Tom$^+$ cells exhibited a significant reduction in E-cadherin expression levels when cultured for 40 h compared to 22 h (Fig. 7C and Figure S13). Additionally, IMT504 induced an overexpression of Wnt5a mRNA levels in Tom$^+$ cells (Figure S13), suggesting the potential involvement of non-canonical Wnt signaling pathways in their increased migratory behavior of GLAST+Wnt1+BMSPs, which requires further investigation. Collectively, these findings indicate that in vitro expanded GLAST+Wnt1+BMSPs possess greater motility capacity than other BMSP subpopulations, and IMT504 significantly enhances their mobilization.

Effect of IMT504 and conditioned media derived from in vitro expanded GLAST+Wnt1+BMSPs on the expression profile of various liver cell types

We finally asked if IMT504 and/or the CM obtained from IMT504 treated Tom$^+$ cells could directly and specifically change the mRNA expression profile of diverse liver cells involved in fibrogenesis. First, primary cultured macrophages that were previously isolated from fibrotic livers were incubated with IMT504 or CM from IMT504-treated Tom$^+$ or Tom$^-$ cells or subjected to other control conditions. Only IMT504 or CM from IMT504-treated Tom$^+$ cells were able to alter the expression profile of these macrophages. Macrophages changed from an inflammatory into a tolerogenic phenotype, characterized by reduction in TNF-α and iNOS levels, and an increase in IL-10 and/or Arginase-1 mRNA levels. Additionally, they acquired a proregenerative phenotype, marked by an increase in HGF, with the IMT504 treatment showing a more pronounced effect compared to CM from IMT504-treated Tom$^+$ cells (Fig. 8).

Under the same experimental conditions, IMT504 and CM from IMT504-treated Tom$^+$ cells were the only stimuli capable of reducing the activation profile of CFSC-2G rat hepatic stellate cells (Fig. 8). Furthermore, they upregulated HGF and IGF-I mRNA expression levels in primary cultured hepatocytes obtained from naïve CD1 mice (Fig. 8), without causing changes in PCNA or β-catenin mRNA expression levels in the latter cell type.

Based on these results, we can conclude that IMT504 has the ability to directly modulate the expression profile of macrophages, hepatic stellate cells and hepatocytes. This suggests that IMT504 could serve as a potent tool for ameliorating liver fibrosis in mouse. Additionally, the increase prevalence of GLAST+Wnt1+BMSP-derived cells caused by IMT504 treatment may also play a role in this context, through paracrine mechanisms.

Discussion

In this study, we demonstrate that IMT504 inhibits the development of liver fibrosis in different in vivo models. Furthermore, it accelerates the regression of established liver fibrosis leading to near-normal conditions. Importantly, we have also shown early parallel mechanisms underlying the beneficial effect of IMT504 in these pathological contexts. The mechanisms triggered by IMT504 seems to be highly complex since as it is now shown it

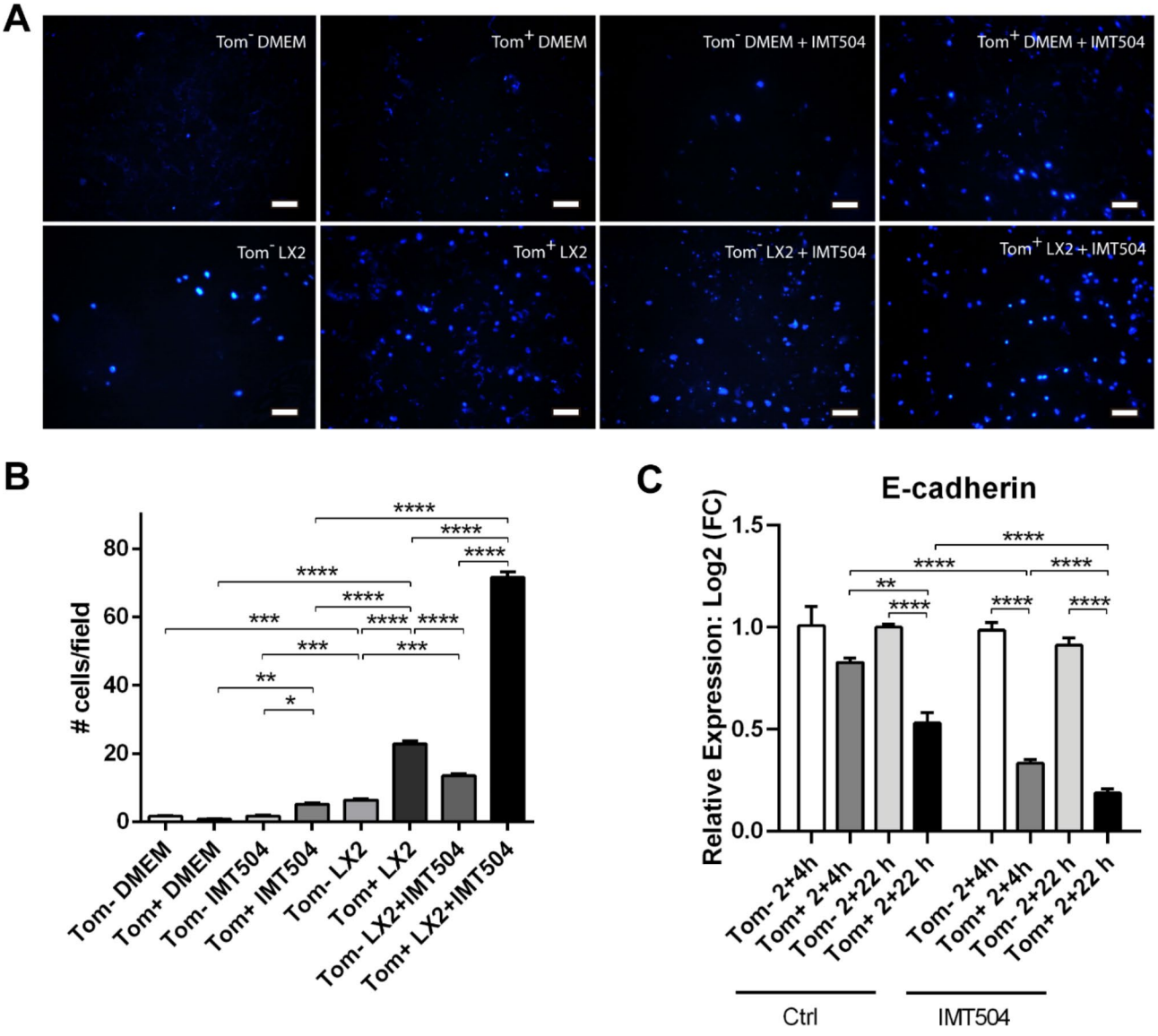

Fig. 7 Effect of IMT504 on the mobilization of P8 GLAST$^+$ Wnt1$^+$ BMSPs. (**A**) Representative images showing DAPI staining on cells which have passed through membrane pores during 4 h in a Boyden chamber assay; scale bars: 50 µm. (**B**) Statistical comparisons of different experimental conditions; Tukey`s multiple comparisons test; $n=5$. (**C**) Statistical comparisons showing changes in E-cadherin expression levels, as measured by qPCR, in between Tom$^+$ and/or Tom$^-$ cells which were pretreated or not with IMT504; $n=3$. (**B, C**) *$p<0,05$; **$p<0,01$; ***$p<0.001$; ****$p<0.0001$; Tukey´s multiple comparisons test

can directly act on fibrotic macrophages, activated hepatic stellate cells, hepatocytes and GLAST$^+$ Wnt1$^+$ BMSPs to change their expression profile.

Within just 1 day after IMT504 subcutaneous administration, the expression profile of the liver undergoes a shift from a pro-inflammatory state to a tolerogenic one. Profibrotic markers are downregulated, and there is a significantly increase in the proliferation and functionality of hepatocytes. The increase in hepatocyte proliferation is probable caused by the reduction in reactive oxygen species (which are known to act during a pro-inflammatory state) and/or the upregulation of HGF and Arginase-1 [37, 38]. Interestingly, these mechanisms closely resemble those previously reported by us following the systemic application of expanded BM stromal cells engineered to produce and deliver IGF-I in the context of liver fibrosis [39]. Moreover, the effect of IMT504 in early-stage and late-stage fibrogenesis were remarkably similar.

Current literature suggests that bone marrow is likely the main source of circulating stromal progenitors with extended plasticity due to its particular hypoxic conditions within the niche microenvironment [40–42]. In

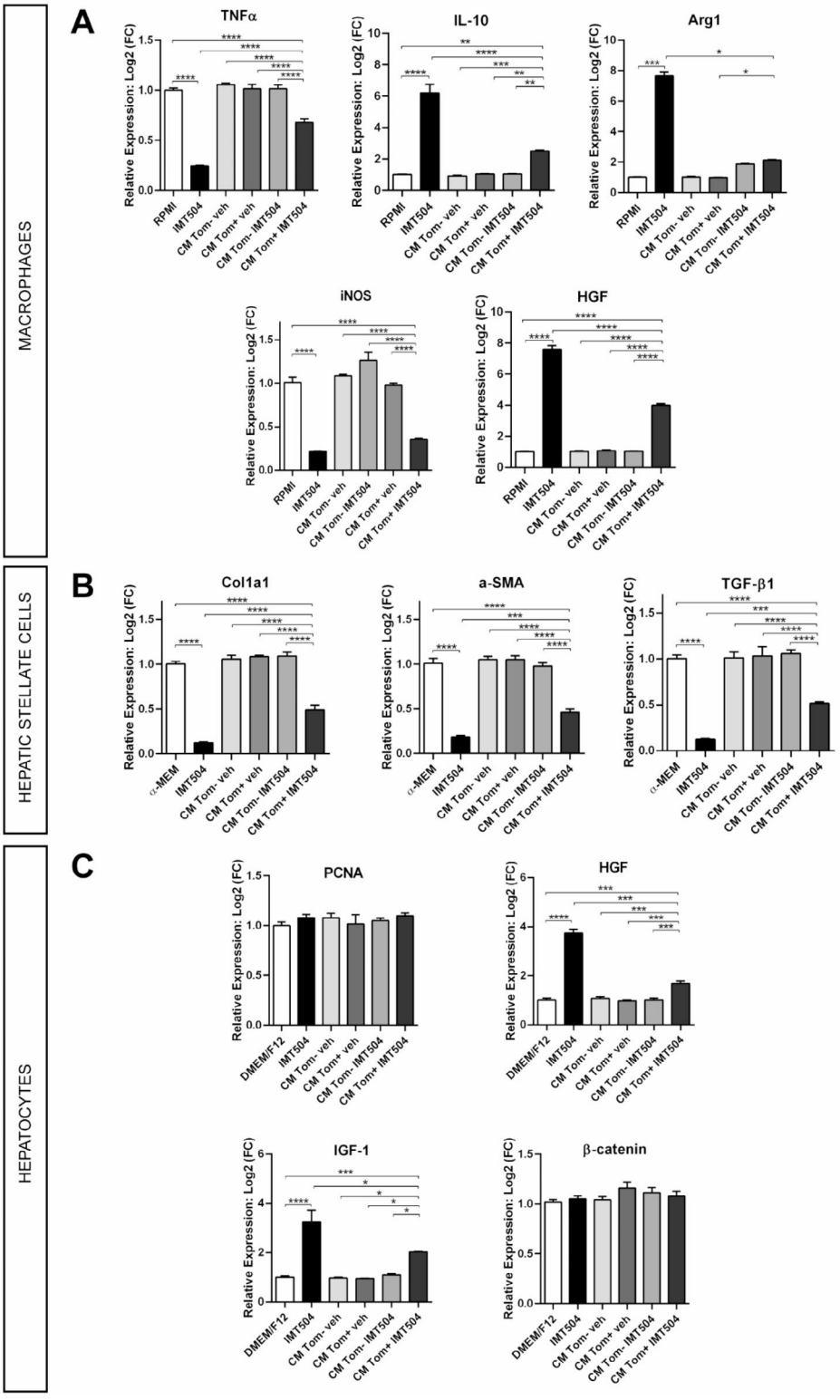

Fig. 8 Effect of IMT504 or conditioned media (CM) from GLAST^{+} Wnt1^{+} BMSPs or Tom^{-} BMSPs treated with IMT504 or vehicle (veh) on the expression pattern of different liver cell populations. (**A**) Statistical comparisons of TNF-α, IL-10, arginase 1, iNOS and HGF mRNA levels in primary cultured macrophages obtained from fibrotic livers (treated with thioacetamide for 6 weeks) after different experimental treatments, as measured by qPCR. (**B**) Statistical comparisons of collagen 1a1, alpha-smooth muscle actin and TGF-β mRNA levels in CFSC-2G cells. (**C**) Statistical comparisons of PCNA, HGF, IGF-I and β-catenin mRNA levels in primary cultured hepatocytes from healthy livers. *$p < 0{,}05$; **$p < 0{,}01$; ***$p < 0.001$; ****$p < 0.0001$; Tukey´s multiple comparisons test; $n = 3$

a previous work, we speculated that circulating Tom$^+$ stromal progenitors in *Wnt1*^{Cre}; *Rosa26*^{Tom} mice may originate in the bone marrow. This is based on the observation that virtually all bone marrow and peripheral blood stromal Tom$^+$ cells express GLAST and CD44. Moreover, there is a shift in the proportion of GLAST$^+$ Wnt1$^+$ CD44$^+$ cells, suggesting mobilization from the bone marrow during liver fibrogenesis and hepatectomy [9]. After 8 weeks of TAA treatment, similar numbers of Tom$^+$ ELCs and HLCs were found in *Wnt1*^{Cre}; *Rosa26*^{Tom} and *GLAST*^{CreERT2}; *Rosa26*^{Tom} (Tx P2) mice [9].

We now provide new evidence demonstrating that GLAST$^+$ Wnt1$^+$ BMSPs are significantly more motile than other BMSPs. Additionally, these cells can acquire ELC and of HLC- specific markers both in vitro and in vivo, likely contributing to endothelial and liver progenitors in the context of liver fibrosis.

Furthermore, we show that IMT504 increases the occurrence and proliferation of Tom$^+$ ELCs and of Tom$^+$ HLCs in *GLAST*^{CreERT2}; *Rosa26*^{Tom} (Tx P2) mice with fibrotic liver. While some contribution from local liver and endothelial progenitors, as well as other tissues, may occur in the context of liver injury and/or IMT504 treatment, it is likely that Tom$^+$ ELCs and Tom$^+$ HLCs at least partially originate from circulating GLAST$^+$ Wnt1$^+$ BMSPs.

We successfully expanded GLAST$^+$ Wnt1$^+$ BMSPs in vitro for several passages. Our current findings reveal that in vivo pretreatment with IMT504 effectively doubled the contribution of GLAST$^+$ Wnt1$^+$ BMSPs to the stromal progenitor fraction, thereby increasing the total number of CFU-Fs. Notably, this ODN significantly influenced the physiological properties of the GLAST$^+$ Wnt1$^+$ BMSPs, particularly in terms of proliferation and motility, while having minimal impact on Wnt1$^-$ BMSPs. Furthermore, naïve GLAST$^+$ Wnt1$^+$ BMSPs exhibit greater motility compared to other BMSP subsets. For this reason, they might hold greater significance in the context of tissue repair mechanisms of different kind, a matter which requires further investigation.

Previously, we reported that TAA inhibited the capacity of GLAST$^+$ Wnt1$^+$ BMSPs to proliferate and form dense colonies [9]. New results suggest that IMT504 can restore the capacity of GLAST$^+$ Wnt1$^+$ BMSPs to generate dense colonies. This finding aligns with the observation that repeated doses of IMT504, administered with a 14 days interval, likely increased the contribution of GLAST$^+$ Wnt1$^+$ BMSPs to liver regeneration.

It is well-established that Wnt signalling plays a significant role in regulating progenitor properties, and canonical Wnt signalling has previously been shown to expand the pool of CFU-Fs in human BMSPs [43]. It is worth noting that at early postnatal stages, within the BMSP fraction, the Wnt1 promoter is active only in a subset of GLAST$^+$ BMSPs [9]. Our new findings reveal that IMT504 specifically targets GLAST$^+$ Wnt1$^+$ BMSPs, leading to an upregulation in Wnt1, Wnt3a and Wnt5a mRNA expression levels, as well as canonical Wnt pathway target genes. Furthermore, our data show that Wnt signaling is required for the IMT504-mediated induction of GLAST$^+$ Wnt1$^+$ BMSPs proliferation.

Notably, previous research has linked Wnt signaling to the acquisition of plastic properties by BM cells. For example, this pathway induced myogenin expression in a subpopulation of mouse BM multipotent adult stem cells (mMASCs), enhancing their capacity to fuse with cocultured skeletal muscle cells, a feature of myocytes [44]. Moreover, Wnt1 was shown to induce the expression of pro-angiogenic factors and drive ELC differentiation in dental pulp stem cells with stromal properties [45]. Furthermore, the activation of Wnt1 signaling was found to be necessary for the differentiation of oval cells into hepatocytes [46]. Further research is required to determine whether GLAST$^+$ Wnt1$^+$ BMSPs may contribute to oval cells and if Wnt signaling is necessary for the increased motility of GLAST$^+$ Wnt1$^+$ BMSPs and their differentiation into or induction of ELC and HLC-specific markers in response to IMT504.

Prior to IMT504 stimulation, both Tom$^+$ or Tom$^-$ cells underwent overnight fetal bovine serum starvation. Following a 2-hours pulse with either ODN or vehicle, they were then allowed to recover for an additional 4–22 h without serum. Notably, both IMT504-treated and untreated Tom$^+$ cells express higher expression levels of Wnt ligands, β-catenin, and various canonical Wnt signalling gene targets, even under conditions of stress such as serum starvation. This observation aligns with expectations, given that GLAST$^+$ Wnt1$^+$ BMSPs are found in proximity to BM sinusoids [9], with low oxygen pressure. Consequently, these cells may possess the ability to perceive subtle alterations in chemoattractant signals in vivo, potentially making them receptive to the influence by IMT504 in expanding the GLAST$^+$ Wnt1$^+$ BMSP population.

In addition, incubation with IMT504 was found to directly influence the expression profiles of various cell types relevant to fibrogenesis and regeneration. Notably, this ODN induced a tolerogenic and proregenerative phenotype in fibrotic macrophages. It also mitigated the activation state of hepatic stellate cells and upregulated the expression of hepatocyte growth factor, which plays a pivotal role in promoting the proliferation and differentiation of progenitors into hepatocytes, as well as IGF-I, a marker of liver cell function, in hepatocytes.

Furthermore, conditioned media from GLAST$^+$ Wnt1$^+$ BMSPs pretreated with IMT504 also exhibited a similar, albeit partial, effect. In contrast, CM from GLAST$^+$ Wnt1$^+$ BMSPs pretreated with vehicle or CM from

Tom$^-$ cells, whether previously exposed to IMT504 or not, did not induce significant changes in the expression profiles of fibrotic macrophages, hepatic stellate cells or hepatocytes. As a result, it is evident that GLAST$^+$ Wnt1$^+$ BMSPs respond uniquely to IMT504 compared to other BMSPs. The impact of IMT504 on the expression profile of GLAST + Wnt1 + BMSPs and its effect on their secretome are yet to be explored. In an in vivo context, these cells are likely to play a pivotal role in mediating the beneficial effects of IMT504 in the context of liver injuries. They may release factors that modulate inflammation and promote regeneration, even after the ODN has been cleared from circulation.

It is worth noting that IMT504 led to an upregulation in Myb, an oncogene, without altering the expression levels of Wnt1 in liver samples enriched with parenchymal cells obtained from mice treated with TAA for 2 and 8 weeks. Notably, neither this ODN nor CM from GLAST$^+$ Wnt1$^+$ BMSPs pre-treated with IMT504 resulted in changes in β-catenin expression levels in primary cultured hepatocytes. This observation may suggest that IMT504 might not induce Wnt1 signaling on hepatocytes, a feature previously involved in carcinogenesis [47–49]. However, it is important to acknowledge that the potential influence of IMT504 on negative mechanisms in the context of cancer remains to be investigated.

Conclusion

In summary, our study underscores the potential of IMT504 in promoting liver repair and fibrosis regression. Its efficacy lies in directly altering the phenotype of fibrotic macrophages, hepatic stellate cells/myofibroblasts, and hepatocytes, pivotal players in liver fibrosis and regeneration. Our work provides new evidences supporting the beneficial effects of IMT504 in promoting recovery in some pathologies involving immune responses. Additionally, IMT504 fosters the proliferation and enhances the contribution of GLAST$^+$ Wnt1$^+$ BMSPs, likely giving rise to HLCs and ELCs. Concurrently, it induces shifts in their secretome, potentially amplifying IMT504's antifibrotic impact.

These GLAST + Wnt1 + BMSPs may engage in similar processes across various tissues, suggesting a broader applicability of IMT504 in different disease contexts. This could signify an evolutionarily conserved mechanism wherein a subset of BMSPs responds to environmental cues, likely involving the Wnt signaling pathway. Such a mechanism could underlie the mobilization of these cells into peripheral blood and their heightened recruitment into injured tissues, where they exert a pro-regenerative function.

Abbreviations

Abl1	Abelson murine leukemia viral oncogene homolog 1
Arg1	Arginase 1
a-SMA	Alpha-smooth muscle actin
α-SMA	Alpha-smooth muscle actin
a1AT	Alpha-1 antitrypsin
α-1AT	Alpha-1 antitrypsin
β-cat	β-catenin
Axn2	Axin 2
BM	Bone marrow
BM-MNCs	Bone marrow mononuclear cells
BMSPs	Bone marrow stromal progenitors
BRCA2	Breast cancer 2
CCNA1	Cyclin A1
CcnD1	Cyclin D1
CFU -F	Fibroblast colony-forming unit
Col1a1	Collagen type I alpha 1 chain
Cre	CRE (causes recombination) recombinase
CreER/CreERT2/CreERTM	CRE recombinase fused to a mutant form of the human estrogen receptor ligand binding domain
ELC	Endothelial-like cell
GADD45A	Growth arrest and DNA-damage-inducible 45α
GLAST	Glutamate-aspartate transporter
GLAST$^+$ Wnt1$^+$ BMSPs	GLAST$^+$ Wnt1-traced bone marrow stromal progenitors
HGF	Hepatocyte growth factor
HLC	Hepatocyte-like cell
IGF-1	Insulin-like growth factor I
IL-1β	Interleukin 1 beta
IL-6	Interleukin 6
IL10	Interleukin 10
iNOS	Inducible nitric oxide synthase
Lef1	Lymphoid enhancer binding factor 1
MSCs	Mesenchymal stem/stromal cells
Myb	Myeloblastosis oncogene
NOTCH2	Notch receptor 2
ODN	Oligodeoxynucleotide
P2/60	Postnatal day 2/60
P8	Passage 8
PCNA	Proliferating cell nuclear antigen
Sp5	Specificity protein 5
TAA	Thioacetamide
TGF-β1	Transforming growth factor-beta 1
TNF-α	Tumor necrosis factor alpha
Tom	tdTomato
TWEAK	Tumor necrosis factor-like weak inducer of apoptosis
Tx	Tamoxifen
vWF	von Willebrand factor
Wnt1	Wingless-type MMTV integration site family, member 1
Wnt3a	Wingless-type MMTV integration site family, member 3 A
Wnt5a	Wingless-type MMTV integration site family, member 5 A

Supplementary Information

The online version contains supplementary material available at https://doi.org/10.1186/s13287-024-03896-w.

Supplementary Material 1

Supplementary Material 2

Supplementary Material 3

Supplementary Material 4

Acknowledgements

We thank Anabel Cañete, Guillermo Gastón, Tobías Giovannetti, Laura Montaldo, Carla Pascuale, Gabriela Periz, Pablo Pomata, Pamela Rodriguez and Paula Roselló for technical support. We are also grateful to Guillermo Lanuza

for experimental suggestions, and Lucia Moro for sharing Wnt inhibitor and activator reactive. Experimental schemes were created with BioRender.com.

Author contributions
MB, RS, MJC, JMBF: conceived and designed the analysis; collected the data; contributed data or analysis tools; performed the analysis. SGB: designed the analysis; collected the data; contributed data or analysis tools. EJF: conceived and designed the analysis; contributed data or analysis tools. GG, MMG, MLR: collected the data; contributed data or analysis tools. MS, JR, AM: contributed data or analysis tools. MGG, GDM: conceived and designed the analysis. JBA: conceived and designed the analysis; collected the data; contributed data or analysis tools; performed the analysis; wrote the manuscript.

Funding
This work has been funded by FONCyT-ANPCyT (PICT-O-2016-0088, PICT-2017-0642 and PICT-2021-I-A-00204) and Austral University.

Data availability
Not applicable. The data supporting the findings of this study are available upon request from the corresponding author.

Declarations

Ethics approval and consent to participate
Human studies or samples were not included. Animal care adhered to NIH ethical guidelines, and the Animal Care Committee from School of Biomedical Sciences, Universidad Austral, approved the experimental protocol (CICUAL IIMT CONICET-Universidad Austral protocols: 2019-03, 2021-06 and 2022-09). Titles of the approved projects: The contribution of the neural crest to liver regeneration (2019-03); Effect of IMT504 on GLAST + Wnt1 + stromal cells from bone marrow in the context of hepatic fibrosis (2021-06); Effect of IMT504 on GLAST + Wnt1 + stromal progenitors from bone marrow in the context of hepatic fibrosis induced by common bile duct ligation (2022-09).

Consent for publication
Not applicable.

Disclosure for use of AI
During the preparation of this work the author(s) used ChatGPT 3.5 in order to improve the language style. After using this tool/service, the authors reviewed and edited the content as needed and take full responsibility for the content of the publication.

Competing interests
The authors declare no competing interests.

Author details
[1]Developmental Biology & Regenerative Medicine Laboratory, Instituto de Investigaciones en Medicina Traslacional, CONICET-Universidad Austral, Derqui, Pilar, Buenos Aires, Argentina
[2]Facultad de Ciencias Biomédicas, Universidad Austral, Pilar, Argentina
[3]Gene Therapy Laboratory, Instituto de Investigaciones en Medicina Traslacional, CONICET- Universidad Austral, Buenos Aires, Argentina
[4]Instituto de Ciencia y Tecnología Dr. César Milstein. Fundación Pablo Cassará, Buenos Aires City, Argentina
[5]Mechanisms and Therapeutic Innovation in Pain Laboratory, Instituto de Investigaciones en Medicina Traslacional, CONICET-Universidad Austral, Buenos Aires, Argentina

Received: 8 May 2024 / Accepted: 23 August 2024
Published online: 04 September 2024

References

1 Aquino JB, Bolontrade MF, Garcia MG, Podhajcer OL, Mazzolini G. Mesenchymal stem cells as therapeutic tools and gene carriers in liver fibrosis and hepatocellular carcinoma. Gene Ther. 2010;17(6):692–708. https://doi.org/10.1038/gt.2010.10.
2 Fiore EJ, Bayo JM, Garcia MG, Malvicini M, Lloyd R, Piccioni F, Rizzo M, Peixoto E, Sola MB, Atorrasagasti C, Alaniz L, Camilletti MA, Enguita M, Prieto J, Aquino JB, Mazzolini G. Mesenchymal stromal cells engineered to produce IGF-I by recombinant adenovirus ameliorate liver fibrosis in mice. Stem Cells Dev. 2015;24(6):791–801. https://doi.org/10.1089/scd.2014.0174.
3 Fiore EJ, Mazzolini G, Aquino JB. Mesenchymal Stem/Stromal cells in liver fibrosis: recent findings, Old/New caveats and Future perspectives. Stem Cell Rev. 2015;11(4):586–97. https://doi.org/10.1007/s12015-015-9585-9.
4 Baccin C, Al-Sabah J, Velten L, Helbling PM, Grunschlager F, Hernandez-Malmierca P, Nombela-Arrieta C, Steinmetz LM, Trumpp A, Haas S. Combined single-cell and spatial transcriptomics reveal the molecular, cellular and spatial bone marrow niche organization. Nat Cell Biol. 2020;22(1):38–48. https://doi.org/10.1038/s41556-019-0439-6.
5 Baryawno N, Przybylski D, Kowalczyk MS, Kfoury Y, Severe N, Gustafsson K, Kokkaliaris KD, Mercier F, Tabaka M, Hofree M, Dionne D, Papazian A, Lee D, Ashenberg O, Subramanian A, Vaishnav ED, Rozenblatt-Rosen O, Regev A, Scadden DT. A Cellular Taxonomy of the bone marrow stroma in Homeostasis and Leukemia. Cell. 2019;177(7):1915–32. https://doi.org/10.1016/j.cell.2019.04.040. e1916.
6 Ilas DC, Baboolal TG, Churchman SM, Jones WG, Giannoudis PV, Buhring HJ, McGonagle D, Jones E. The osteogenic commitment of CD271 + CD56 + bone marrow stromal cells (BMSCs) in osteoarthritic femoral head bone. Sci Rep. 2020;10(1):11145. https://doi.org/10.1038/s41598-020-67998-0.
7 Tikhonova AN, Dolgalev I, Hu H, Sivaraj KK, Hoxha E, Cuesta-Dominguez A, Pinho S, Akhmetzyanova I, Gao J, Witkowski M, Guillamot M, Gutkin MC, Zhang Y, Marier C, Diefenbach C, Kousteni S, Heguy A, Zhong H, Fooksman DR, Aifantis I. The bone marrow microenvironment at single-cell resolution. Nature. 2019;569(7755):222–8. https://doi.org/10.1038/s41586-019-1104-8.
8 Zhao M, Tao F, Venkatraman A, Li Z, Smith SE, Unruh J, Chen S, Ward C, Qian P, Perry JM, Marshall H, Wang J, He XC, Li L. N-Cadherin-expressing bone and marrow stromal progenitor cells maintain Reserve hematopoietic stem cells. Cell Rep. 2019;26(3):652–e669656. https://doi.org/10.1016/j.celrep.2018.12.093.
9 Sierra R, Gomez Bustillo S, Kameneva P, Fiore EJ, Mazzone GL, Borda M, Blanco MV, Usuardi C, Furlan A, Ernfors P, Alaniz L, Montaner AD, Adameyko I, Aquino JB. Contribution of neural crest and GLAST(+) Wnt1(+) bone marrow pericytes with liver fibrogenesis and/or regeneration. Liver Int. 2020. https://doi.org/10.1111/liv.14401.
10 Bao J, Wu Q, Wang Y, Li Y, Li L, Chen F, Wu X, Xie M, Bu H. Enhanced hepatic differentiation of rat bone marrow-derived mesenchymal stem cells in spheroidal aggregate culture on a decellularized liver scaffold. Int J Mol Med. 2016;38(2):457–65. https://doi.org/10.3892/ijmm.2016.2638.
11 Oh SH, Witek RP, Bae SH, Zheng D, Jung Y, Piscaglia AC, Petersen BE. Bone marrow-derived hepatic oval cells differentiate into hepatocytes in 2-acetylaminofluorene/partial hepatectomy-induced liver regeneration. Gastroenterology. 2007;132(3):1077–87. https://doi.org/10.1053/j.gastro.2007.01.001.
12 Piryaei A, Valojerdi MR, Shahsavani M, Baharvand H. Differentiation of bone marrow-derived mesenchymal stem cells into hepatocyte-like cells on nanofibers and their transplantation into a carbon tetrachloride-induced liver fibrosis model. Stem Cell Rev Rep. 2011;7(1):103–18. https://doi.org/10.1007/s12015-010-9126-5.
13 Sato Y, Araki H, Kato J, Nakamura K, Kawano Y, Kobune M, Sato T, Miyanishi K, Takayama T, Takahashi M, Takimoto R, Iyama S, Matsunaga T, Ohtani S, Matsuura A, Hamada H, Niitsu Y. Human mesenchymal stem cells xenografted directly to rat liver are differentiated into human hepatocytes without fusion. Blood. 2005;106(2):756–63. https://doi.org/10.1182/blood-2005-02-0572.
14 Krieg AM, Yi AK, Matson S, Waldschmidt TJ, Bishop GA, Teasdale R, Koretzky GA, Klinman DM. CpG motifs in bacterial DNA trigger direct B-cell activation. Nature. 1995;374(6522):546–9. https://doi.org/10.1038/374546a0.
15 Elias F, Flo J, Lopez RA, Zorzopulos J, Montaner A, Rodriguez JM. Strong cytosine-guanosine-independent immunostimulation in humans and other primates by synthetic oligodeoxynucleotides with PyNTTTTGT motifs. J Immunol. 2003;171(7):3697–704. https://doi.org/10.4049/jimmunol.171.7.3697.
16 Hernando Insúa A, Montaner AD, Rodriguez JM, Elías F, Fló J, López RA, Zorzopulos J, Hofer EL, Chasseing NA. IMT504, the prototype of the immunostimulatory oligonucleotides of the PyNTTTTGT class, increases the number of progenitors of mesenchymal stem cells both in vitro and in vivo: potential use in tissue repair therapy. Stem Cells. 2007;25(4):1047–54. https://doi.org/10.1634/stemcells.2006-0479.
17 Zorzopulos J, Opal SM, Hernando-Insúa A, Rodriguez JM, Elías F, Fló J, López RA, Chasseing NA, Lux-Lantos VA, Coronel MF, Franco R, Montaner AD, Horn DL. Immunomodulatory oligonucleotide IMT504: effects on mesenchymal stem cells as a first-in-class immunoprotective/immunoregenerative therapy. World J Stem Cells. 2017;9(3):45–67. https://doi.org/10.4252/wjsc.v9.i3.45.

18 Bianchi MS, Hernando-Insua A, Chasseing NA, Rodriguez JM, Elias F, Lago N, Zorzopulos J, Libertun C, Montaner AD, Lux-Lantos VA. Oligodeoxynucleotide IMT504 induces a marked recovery in a streptozotocin-induced model of diabetes in rats: correlation with an early increase in the expression of nestin and neurogenin 3 progenitor cell markers. Diabetologia. 2010;53(6):1184–9. https://doi.org/10.1007/s00125-010-1694-z.

19 Bianchi S, Martinez Allo VC, Massimino M, Lavignolle Heguy MDR, Borzone FR, Bustillo G, Chasseing S, Libertun NA, Montaner C, Rabinovich AD, Toscano GA, Lux-Lantos MA, V. A., Bianchi MS. Oligonucleotide IMT504 improves glucose metabolism and Controls Immune Cell mediators in Female Diabetic NOD mice. Nucleic Acid Ther. 2021;31(2):155–71. https://doi.org/10.1089/nat.2020.0901.

20 Casadei M, Fiore E, Rubione J, Dominguez LM, Coronel MF, Leiguarda C, Garcia M, Mazzolini G, Villar MJ, Montaner A, Constandil L, Romero-Sandoval EA, Brumovsky PR. IMT504 blocks allodynia in rats with spared nerve injury by promoting the migration of mesenchymal stem cells and by favoring an anti-inflammatory milieu at the injured nerve. Pain. 2022;163(6):1114–29. https://doi.org/10.1097/j.pain.0000000000002476.

21 Mathieu PA, Sampertegui YR, Elias F, Silva AS, de Lujan Calcagno M, Lopez R, Adamo AM. Oligodeoxynucleotide IMT504: effects on Central Nervous System Repair following demyelination. Mol Neurobiol. 2023. https://doi.org/10.1007/s12035-023-03825-7.

22 Mori T, Tanaka K, Buffo A, Wurst W, Kuhn R, Gotz M. Inducible gene deletion in astroglia and radial glia–a valuable tool for functional and lineage analysis. Glia. 2006;54(1):21–34. https://doi.org/10.1002/glia.20350.

23 Tag CG, Sauer-Lehnen S, Weiskirchen S, Borkham-Kamphorst E, Tolba RH, Tacke F, Weiskirchen R. Bile duct ligation in mice: induction of inflammatory liver injury and fibrosis by obstructive cholestasis. J Vis Exp. 2015;96. https://doi.org/10.3791/52438.

24 Gomez GA, Prasad MS, Sandhu N, Shelar PB, Leung AW, Garcia-Castro MI. Human neural crest induction by temporal modulation of WNT activation. Dev Biol. 2019;449(2):99–106. https://doi.org/10.1016/j.ydbio.2019.02.015.

25 Martins-Neves SR, Paiva-Oliveira DI, Fontes-Ribeiro C, Bovee J, Cleton-Jansen AM, Gomes CMF. IWR-1, a tankyrase inhibitor, attenuates Wnt/beta-catenin signaling in cancer stem-like cells and inhibits in vivo the growth of a subcutaneous human osteosarcoma xenograft. Cancer Lett. 2018;414:1–15. https://doi.org/10.1016/j.canlet.2017.11.004.

26 Tang H, Xu Y, Zhang Z, Zeng S, Dong W, Jiao W, Hu X. SDF–1/CXCR4 induces epithelial–mesenchymal transition through activation of the Wnt/beta–catenin signaling pathway in rat chronic allograft nephropathy. Mol Med Rep. 2019;19(5):3696–706. https://doi.org/10.3892/mmr.2019.10045.

27 Blas-Garcia A, Apostolova N. Novel therapeutic approaches to liver fibrosis based on targeting oxidative stress. Antioxid (Basel). 2023;12(8). https://doi.org/10.3390/antiox12081567.

28 Rountree CB, Barsky L, Ge S, Zhu J, Senadheera S, Crooks GM. A CD133-expressing murine liver oval cell population with bilineage potential. Stem Cells. 2007;25(10):2419–29. https://doi.org/10.1634/stemcells.2007-0176.

29 Thomas JA, Pope C, Wojtacha D, Robson AJ, Gordon-Walker TT, Hartland S, Ramachandran P, Van Deemter M, Hume DA, Iredale JP, Forbes SJ. Macrophage therapy for murine liver fibrosis recruits host effector cells improving fibrosis, regeneration, and function. Hepatology. 2011;53(6):2003–15. https://doi.org/10.1002/hep.24315.

30 Golestaneh N, Beauchamp E, Fallen S, Kokkinaki M, Uren A, Dym M. Wnt signaling promotes proliferation and stemness regulation of spermatogonial stem/progenitor cells. Reproduction. 2009;138(1):151–62. https://doi.org/10.1530/REP-08-0510.

31 Ikeya M, Lee SM, Johnson JE, McMahon AP, Takada S. Wnt signalling required for expansion of neural crest and CNS progenitors. Nature. 1997;389(6654):966–70. https://doi.org/10.1038/40146.

32 Morgan-Smith M, Wu Y, Zhu X, Pringle J, Snider WD. GSK-3 signaling in developing cortical neurons is essential for radial migration and dendritic orientation. Elife. 2014;3:e02663. https://doi.org/10.7554/eLife.02663.

33 Reya T, Clevers H. Wnt signalling in stem cells and cancer. Nature. 2005;434(7035):843–50. https://doi.org/10.1038/nature03319.

34 Tetsu O, McCormick F. Beta-catenin regulates expression of cyclin D1 in colon carcinoma cells. Nature. 1999;398(6726):422–6. https://doi.org/10.1038/18884.

35 Bayo J, Fiore E, Aquino JB, Malvicini M, Rizzo M, Peixoto E, Alaniz L, Piccioni F, Bolontrade M, Podhajcer O, Garcia MG, Mazzolini G. (2014). Human umbilical cord perivascular cells exhibited enhanced migration capacity towards hepatocellular carcinoma in comparison with bone marrow mesenchymal stromal cells: a role for autocrine motility factor receptor. *Biomed Res Int*, *2014*, 837420. https://doi.org/10.1155/2014/837420

36 Yue Z, Yuan Z, Zeng L, Wang Y, Lai L, Li J, Sun P, Xue X, Qi J, Yang Z, Zheng Y, Fang Y, Li D, Siwko S, Li Y, Luo J, Liu M. LGR4 modulates breast cancer initiation, metastasis, and cancer stem cells. FASEB J. 2018;32(5):2422–37. https://doi.org/10.1096/fj.201700897R.

37 Nishikoba N, Kumagai K, Kanmura S, Nakamura Y, Ono M, Eguchi H, Kamibayashiyama T, Oda K, Mawatari S, Tanoue S, Hashimoto S, Tsubouchi H, Ido A. HGF-MET signaling shifts M1 macrophages toward an M2-Like phenotype through PI3K-Mediated induction of Arginase-1 expression. Front Immunol. 2020;11:2135. https://doi.org/10.3389/fimmu.2020.02135.

38 Sharma P, Nandave M, Nandave D, Yadav S, Vargas-De-La-Cruz C, Singh S, Tandon R, Ramniwas S, Behl T. Reactive oxygen species (ROS)-mediated oxidative stress in chronic liver diseases and its mitigation by medicinal plants. Am J Transl Res. 2023;15(11):6321–41. https://www.ncbi.nlm.nih.gov/pubmed/38074830.

39 Fiore E, Malvicini M, Bayo J, Peixoto E, Atorrasagasti C, Sierra R, Rodriguez M, Gomez Bustillo S, Garcia MG, Aquino JB, Mazzolini G. Involvement of hepatic macrophages in the antifibrotic effect of IGF-I-overexpressing mesenchymal stromal cells. Stem Cell Res Ther. 2016;7(1):172. https://doi.org/10.1186/s13287-016-0424-y.

40 Aquino JB, Sierra R, Montaldo LA. Diverse cellular origins of adult blood vascular endothelial cells. Dev Biol. 2021;477:117–32. https://doi.org/10.1016/j.ydbio.2021.05.010.

41 He Q, Wan C, Li G. Concise review: multipotent mesenchymal stromal cells in blood. Stem Cells. 2007;25(1):69–77. https://doi.org/10.1634/stemcells.2006-0335.

42 Hong HS, Lee J, Lee E, Kwon YS, Lee E, Ahn W, Jiang MH, Kim JC, Son Y. A new role of substance P as an injury-inducible messenger for mobilization of CD29(+) stromal-like cells. Nat Med. 2009;15(4):425–35. https://doi.org/10.1038/nm.1909.

43 Baksh D, Tuan RS. Canonical and non-canonical wnts differentially affect the development potential of primary isolate of human bone marrow mesenchymal stem cells. J Cell Physiol. 2007;212(3):817–26. https://doi.org/10.1002/jcp.21080.

44 Bedada FB, Gunther S, Kubin T, Braun T. Differentiation versus plasticity: fixing the fate of undetermined adult stem cells. Cell Cycle. 2006;5(3):223–6. https://doi.org/10.4161/cc.5.3.2364.

45 Zhang Z, Nor F, Oh M, Cucco C, Shi S, Nor JE. Wnt/beta-Catenin signaling determines the vasculogenic fate of postnatal mesenchymal stem cells. Stem Cells. 2016;34(6):1576–87. https://doi.org/10.1002/stem.2334.

46 Williams JM, Oh SH, Jorgensen M, Steiger N, Darwiche H, Shupe T, Petersen BE. The role of the wnt family of secreted proteins in rat oval stem cell-based liver regeneration: Wnt1 drives differentiation. Am J Pathol. 2010;176(6):2732–42. https://doi.org/10.2353/ajpath.2010.080486.

47 Khemlina G, Ikeda S, Kurzrock R. The biology of hepatocellular carcinoma: implications for genomic and immune therapies. Mol Cancer. 2017;16(1):149. https://doi.org/10.1186/s12943-017-0712-x.

48 Lee HC, Kim M, Wands JR. Wnt/Frizzled signaling in hepatocellular carcinoma. Front Biosci. 2006;11:1901–15. https://doi.org/10.2741/1933.

49 Xu C, Xu Z, Zhang Y, Evert M, Calvisi DF, Chen X. beta-catenin signaling in hepatocellular carcinoma. J Clin Invest. 2022;132(4). https://doi.org/10.1172/JCI154515.

Publisher's note